Check for updates

Advances in electrospun chitosan nanofiber biomaterials for biomedical applications

Ganesan Padmini Tamilarasi, [iD] [a] Govindaraj Sabarees, [iD] [b] Krishnan Manikandan,*[a] Siddan Gouthaman, [iD] [c] Veerachamy Alagarsamy [iD] *[d] and Viswas Raja Solomon [iD] *[d]

Chitosan demonstrates exceptional qualities that enable a variety of applications. Because of this, chitosan-based biomaterials have been produced over time and have the potential to drastically alter the material's properties, leading to the development of unique features. Chitosan is a biopolymer from renewable resources obtained from crabs, lobsters, turtles, shrimp, insects, and food waste. Its exceptional qualities make it a desirable choice for many currently interesting applications. Chitosan is a peculiar type of biopolymer, and the presence of primary amines throughout its backbone structure gives it advantageous physicochemical characteristics and unique interactions with proteins, cells, and other living things. It offers several inherently beneficial qualities, including non-toxicity, antibacterial activity, and biodegradability. The most well-known, influential, and commonly used method for creating chitosan nanofibers is electrospinning. These nanofibers are emerging materials in the biological sectors because of their many benefits, including enhanced porosity, mechanical properties, improved surface functions, high surface area, multi-scale pore size distribution, and intrinsic beneficial features. One of the quickest-growing areas in the life sciences, functionalized chitosan-based electrospun nanofiber research, has recently produced novel drug delivery systems and enhanced scaffolds for regenerative medicine, wound dressings, and antibacterial coatings. Here, we critically review the evolution of CS-based nanofibers and talk about recent advancements in several biomedical fields, emphasizing discoveries and research findings. According to numerous research studies, chitosan nanofibers are ideal materials for various biomedical applications.

1. Introduction

Sustainable nanotechnology's future depends on breaking down scientific hurdles to invent new principles and properly addressing environmental and socioeconomic problems, particularly in large-scale material manufacturing. The most significant issues in this regard are the increased usage of "green" materials (in terms of the chemistry involved) in producing nanoscale-based goods. Natural biopolymers often have higher biocompatibility than synthetic materials and are thus better suited for usage in the human body.[1,2]

Chitosan is now one of the most appealing and environmentally acceptable natural biopolymers due to its accessibility, digestibility, bacteriostatic and anti-inflammatory properties, biocompatibility, and biodegradability. Chitin, the precursor of chitosan, is obtained from the shells of crustaceans such as crabs, lobsters, shrimp, prawns, and mushrooms using various processing techniques that include demineralization and deproteinization.[3–5] The chitin is subsequently partially or completely deacetylated to produce chitosan. Two monomers, β-(1-4)-2-acetamino-2-deoxy-β-D-glucose (N-acetyl-D-glucosamine) and β-(1-4)-2-deoxy β-D-glucopyranose, make up the rigid D-glucosamine repeat (N-amino-D-glucosamine) unit of chitosan.[6] Each subunit of chitosan contains amine, primary hydroxyl, and secondary hydroxyl functional groups. The amino acids are often the subject of chemical changes to produce desired characteristics and unique biological activities. The ratio of N-amino-D-glucosamine to N-acetyl-D-glucosamine, known as the degree of deacetylation (DDA) of chitosan, is a crucial marker for distinguishing between chitin and chitosan and the source of chitosan's unique features. The polymer, also known as chitosan, is dissolved in aqueous acidic conditions when the DDA exceeds 50%. Since the amino groups have been protonated, it is regarded as a cationic biopolymer. A high DDA improves compatibility and boosts interaction with chitosan and cells regarding the biological activity.[7,8]

[a] Department of Pharmaceutical Analysis, SRM College of Pharmacy, SRM Institute of Science and Technology, Kattankulathur, Chennai 603203, India

[b] Department of Pharmaceutical Chemistry, SRM College of Pharmacy, SRM Institute of Science and Technology, Kattankulathur, Chennai 603203, India

[c] Organic Material Laboratory, Department of Chemistry, Indian Institute of Technology, Roorkee 247667, India

[d] Medicinal Chemistry Research Laboratory, MNR College of Pharmacy, Greater Hyderabad, Sangareddy 502294, India. E-mail: vrajasolomon@gmail.com
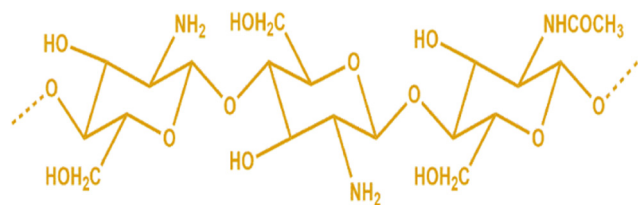
Fig. 1 Molecular structure of chitosan.

Chitosan is chitin's *N*-deacetylation product (Fig. 1). The condensation of glucosamine forms the ideal chitosan structure. It has a complicated double helix structure with 0.5 nm pitch and 6 sugar residues in each helix plane. Because of the abundance of $-OH$, $-O-$, and $-NH_2$ groups, its structure contains numerous intramolecular and intermolecular hydrogen bonds.[9,10] Chitosan may be classified as low (50 kDa), medium (50–150 kDa), or high molecular weight (>150 kDa), depending on its molecular weight. A shift in the molecular weight affects the properties of chitosan, including its solubility, permeability, viscosity, and crystal structure. Permeation and mucoadhesion also improve substantially when chitosan's molecular weight rises. The deacetylation level of commercially available chitosan ranges from 40% to 98%.[11,12] Chitosan gains higher elasticity and flexibility when the deacetylation levels rise, and the intramolecular hydrogen connections within the chain also become more robust.[13,14] Chitosan is insoluble in alkaline or neutral pH due to the weak essential character of D-glucosamine fragments, which have a pK_a between 6.2 and 7, but are soluble in acidic pH (about pH 6). With constant stirring, chitosan dissolves in hydrochloric acid, formic acid, acetic acid, succinic acid, citric acid, lactic acid, and tartaric acid.[15] In polyanionic chemicals, chitosan forms aggregates, while chelates are created when heavy metals are present. Due to its ability to aggregate and be dissolved in acidic solutions, chitosan is an effective gel-forming agent.[16] The viscosity of the chitosan solution is directly related to the amount of deacetylation in the aqueous solution, which causes conformational changes. At high deacetylation, charge repulsion increases viscosity. The viscosity of the solution is also shown to rise with increasing chitosan content. Nevertheless, it falls off when the temperature drops. Since diverse biomedical applications need viscosities of various consistencies, chitosan's viscosity is significant. Another crucial aspect is that chitosan solutions become viscous even at modest concentrations, making it challenging to electro-spin the material into nanofibers. Combining chitosan with other polymers is advised to get around this.[17] Functional groups on the chitosan, specifically the reactive $-OH$ and $-NH_2$ groups, are the principal targets for chemical alterations of chitosan.[18,19] Modified chitosan has improved natural properties like bioactivity, biodegradability, biocompatibility, nontoxicity, and environmental friendliness without sacrificing its natural medicinal properties.[20,21] As a result, chitosan derivatives are effectively used as a vehicle or carrier for the targeted delivery of medications to the desired targets.[22,23] Many studies have shown the environmental friendliness, biocompatibility, sustainability, and multifunctionality of chitosan and its derivatives.[24] Similarly, several exploratory and biological research studies showed that chitosan is safe for biomedical applications and biodegradable *in vivo*. This is supported by research demonstrating how human enzymes, namely lysozyme, degrade chitosan, demonstrating its biodegradable nature.[25] Due to similarities in content and structure between chitosan and the glycosaminoglycans found in human tissues, chitosan causes a mild immunological reaction when it comes into contact with people. Chitosan is one of the most thoroughly studied biomacromolecules, and it has attracted much interest due to its wide range of biomedical uses.[26] The numerous cations on the amino groups of chitosan and the anions of a mucus layer that resembles a gel produce the mucoadhesive joint. Several physicochemical characteristics of chitosan may also impact how mucoadhesive it is. Lehr *et al.* findings suggest that higher-molecular-weight chitosan exhibits a comparably more fantastic mucoadhesive property.[27] Interestingly, some research has shown that trimethylating and PEGylating chitosan increase their mucoadhesive strength by around 3.4 times.[28] Research shows that thiolated chitosan is a desirable mucoadhesive polymer for bioadhesive drug administration. It helps regulate medication distribution and can improve penetration while shielding the drug from deteriorating enzymes.[29,30] Chitosan is utilized for specific applications due to its various biological activities, which include antibacterial, antithrombogenic, antitumor, antifungal, immunoadjuvant, anticholesteremic, and bioadhesive properties.[31] These biopolymers have extensive applications as absorption enhancers and moisturizing agents, in addition to their utility in film manufacturing, tissue regeneration, and wound management.[32] Chitosan can be a drug delivery agent *via* oral, nasal, and ocular routes in implantable and injectable forms.[33] Depending on the intended application, chitosan can be processed into various conformations, including solutions, gels, powders, capsules, films, beads, sponges, and fibers.[34] Therefore, chitosan is primarily used for tissue engineering and wound care dressings. Chitosan-based materials offer several advantages, including biodegradability, antibacterial activity, hydrophilic properties, and polar groups that can form secondary interactions with other polymers. These interactions involve $-OH$ and $-NH_2$ groups participating in hydrogen bonding and *N*-acetyl groups engaging in hydrophobic interactions.[35,36] The mucoadhesive properties of chitosan and its cationic derivatives have been scientifically demonstrated to improve drug absorption, particularly under neutral pH conditions. *N*-Trimethyl chitosan chloride exhibits an interaction with cell membranes that are negatively charged. The transmucosal absorption promotion effect of chitosan is noteworthy for the nasal and oral administration of polar drugs, particularly for the delivery of peptides and proteins and vaccine delivery. Chitosan microspheres with porous structures were fabricated for controlled delivery of antigens. As mentioned, the article encapsulated the Newcastle disease virus vaccine and was subsequently subjected to *in vitro* and *in vivo* testing.[37] The amphiphilic polymer, *N*-lauryl-carboxymethyl chitosan, can form micelles that effectively solubilize taxol, increasing efficiency. This particular chitosan derivative has been deemed safe regarding membrane toxicity and may serve as a beneficial vehicle for hydrophobic cancer medications.[38]

Considerable emphasis has been placed on the hydroxyapatite–chitosan composite material, which has potential applications as a bone-filling material for guided tissue regeneration. A promising application of chitosan–calcium phosphate cement has been discovered. A mixture of chitosan or chitosan glycerophosphate, calcium phosphate, and citric acid resulted in the development of an injectable self-hardening system suitable for bone repair or filling applications.[39,40] Chitosan or its derivatives have been utilized for gene transfection, and the results indicate that the transfection efficiency of N-alkylated chitosan and quaternized chitosan is positively correlated with the length of the alkyl side chains, up to eight carbons in length.

Chitosan, a polycationic substance considered pseudo-natural, is utilized in the creation of electrostatic complexes with both synthetic and natural polymers such as alginate. These complexes are commonly employed as anti-thrombogenic materials for controlled release, encapsulation of drugs, immobilization of enzymes and cells, and as gene carriers.[41] Chitosan has been observed to expedite the process of wound healing when administered through spray, gel, or gauze. This substance is utilized to provide support to medications or regulate drug release. Its properties include cytocompatibility, nontoxicity, biodegradability, mechanical suitability, physiological inertness, antibacterial characteristics, hydrophilic nature, gel-forming abilities, protein affinity, and mucoadhesiveness. Chitosan's molecular weight and functional groups play a significant role in inhibiting bacterial and fungal growth. Small oligomeric chitosan, as opposed to large molecular weight chitosan, can quickly enter the cell membrane of a bacterium, preventing cell development by blocking RNA transcription.[42] Developing materials for wound dressing and tissue engineering is crucial yet ongoing. Lastly, the text highlights various instances where tissue engineering and drug delivery have been applied. Chitosan can be processed more efficiently than chitin in various forms, such as sponges, capsules, or nanoparticles, depending on the specific system being tested and the intended purpose of its administration.

In contrast to a high DDA, a low DDA causes an increase in the release of osteoprotegerin and sclerostin. Furthermore, compared to chitosan with a comparable DDA but a lower molecular weight (MW), a high DDA and high MW have been demonstrated to enhance the secretion of vascular endothelial growth factor and interleukin-6, but decrease osteopontin secretion. Therefore, altering DDA and MW gives a method to modify chitosan to meet specific industrial or medicinal needs. On the other hand, deacetylation removes acetyl groups, altering MW, which must be considered when developing chitosan-based products.[43,44] For example, MW may change chitosan's antibacterial characteristics, which affect bacterial physiological functions at the cellular level, the MW of chitosan, often ranging from 300 to 1 million kDa, is also a factor. Molecules with a low MW and DDA are much more reactive than substrates but more susceptible to biological and chemical decay. Molecules with a lower MW degrade more quickly than those with a higher molecular weight.[45]

Today, one of the unique processes for making nanofibers is electrospinning. Compared to other methods, electrospinning is efficient for creating polymeric fibers that are sub-micron or nanoscale in size. It also has several advantages, including the ease with which bioactive compounds can be incorporated into the nanofibers and the lack of heat during the process, which is crucial for sensitive materials. Electrospun nanofibers are a novel class of materials with several potential applications in the biomedical sector.[46] Chitosan nanofibers are produced using the unique technology of electrospinning. Due to their high porosity and surface area, these nanofibers are ideal for biomedical applications. The electrospun chitosan-based nanofibers produced had unusual properties such as a high surface area to volume ratio, high porosity, and tiny pore size. Due to these characteristics, these nanofibers may be used for various purposes, such as tissue engineering, medication delivery, wound dressing, and membranes.[47] The resulting electrospun nanofibers may be improved, or their material diversity increased using various techniques. The easiest method has been determined to be surface coating, in particular. Due to their structural and chemical resemblance to the natural ECM, chitosan nanofibers are particularly common in tissue regeneration. The nanostructure closely resembles the ECM and offers more surface area for the delivery of biotherapeutics.[48,49] The electrospun nanofibers' porous structure and high specific surface area make them excellent for use in various potential applications, such as drug delivery, bioengineering, surgical equipment, dental fillings, and cosmetics. Another important use for nanofibers is anticipated to be in filtration, metal ion recovery, catalysts, protective clothing, and power storage.[50] This review paper aims to summarise and discuss the recent developments in different biomedical applications of electrospun chitosan, emphasizing electrospun nanofibers.

2. Extraction and purification of chitosan

Chitin, the second-largest natural source of polysaccharides in the shells of living things, including crabs, lobsters, turtles, shrimp, and insects, is the source of chitosan.[51] Researchers have created and put forward several ways to extract chitosan from the shells of various crustaceans, insects, and fungi over the years.[52] First, to remove the protein, the dried shells of crustaceans are treated with an alkali solution, e.g., KOH, NaOH, etc. Second, deproteinized shells were treated with a diluted solution of a mineral acid such as HCl to remove minerals. The chitin is decolored by treating the resulting chitin with an oxidizing agent such as $KMnO_4$, H_2O_2, etc., then washing it with an oxalic acid solution. The result is referred to as "pure chitin." The decolorized chitin is then deacetylated to turn into chitosan by soaking it in a robust alkali solution for several hours. The resulting chitosan fraction is then dried and stored at room temperature. The raw chitosan is treated with aqueous 2% (w/v) acetic acid to produce the cleanest form. This solution is then neutralized with NaOH to create a pure chitosan sample as a white residue that may be transformed into beads or powders.[53,54] Chitosan may need to be cleaned before it can be used in medicine and pharmaceuticals (Fig. 2). Most of the chitosan sold commercially has deacetylation values between 70%
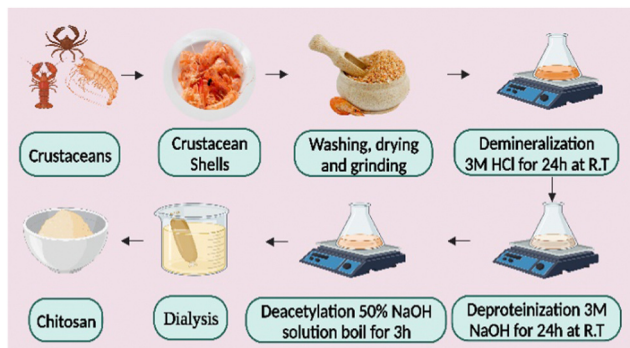
Fig. 2 A diagrammatic illustration of the extraction of chitosan from a crustacean exoskeleton.

and 90%; Chitosan may even attain deacetylation values as high as 95% with further deacetylation procedures. Although this may partially degrade the polymer chains and thus increase the likelihood of deacetylation, the amount of deacetylation affects the molecular weight of chitosan. The rate of deacetylation is slower for molecules with a higher molecular weight, which makes them more chemically stable and more robust but less soluble in traditional solvents to prevent any unfavorable side effects. The deacetylation of chitin is often carried out in a nitrogen atmosphere or with the addition of sodium borohydride to the NaOH solution. Chitosan has an average molecular weight of 1.2×10^5 gmol^{-1}.[55]

3. Electrospun chitosan nanofibers and factors influencing fiber morphology

Electrospinning is the technology used to produce nanofibers most frequently because of its straightforward setup. In a typical electrospinning setup, a grounded collector, a spinneret, and a high-voltage power supply are used (Fig. 3).[56,57] Electrodes join the collector and spinneret to complete the circuit, which creates the electric field. A precursor solution—typically a polymer, sol–gel, or melt—is added to the spinneret and advanced at a slow feed rate to produce a pendant drop held at the tip of the spinneret by surface tension. As the voltage rises due to the repelling of electrical forces, the pendant drop is drawn into a conical shape, known as a Taylor Cone. The Taylor Cone erupts with a liquid jet. The voltage must rise to a certain point before electrical forces triumph over surface tension
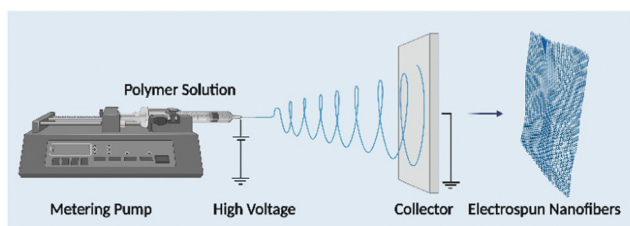
forces, which takes 18 nanoseconds. The liquid spray is stretched and whipped because of the polymeric solution's bending instability, which also causes the solvent to evaporate before the fibers are gathered on the target.[58]

Equipment for electrospinning is currently being commercialized quickly. Fig. 4 and 5 represent the different types of electrospinning and main surface modification techniques used to improve the surface nanofibre properties. Different types of electrospinning techniques have been developed to circumvent the limitations of the traditional electrospinning method (Table 1).

Chitosan is challenging to make into a submicron-sized fibrous form because of its rigid D-glucosamine repeat units and propensity to establish inter or intramolecular hydrogen bonds, resulting in low solubility in pure water and other ordinary organic solvents. Because primary amines are protonated when the pH is lowered, it has been shown that chitosan is more water-soluble.[59] Chitosan's solubility in aqueous acidic solutions is increased by the formation of inter-chain hydrogen bonds with water molecules, which are prevented from occurring by the electrostatic repulsive interactions between positive ammonium groups. The most typical pH adjustment agent has been acetic acid. Pure chitosan has been successfully electrospun using a solvent with a high concentration of acetic acid in

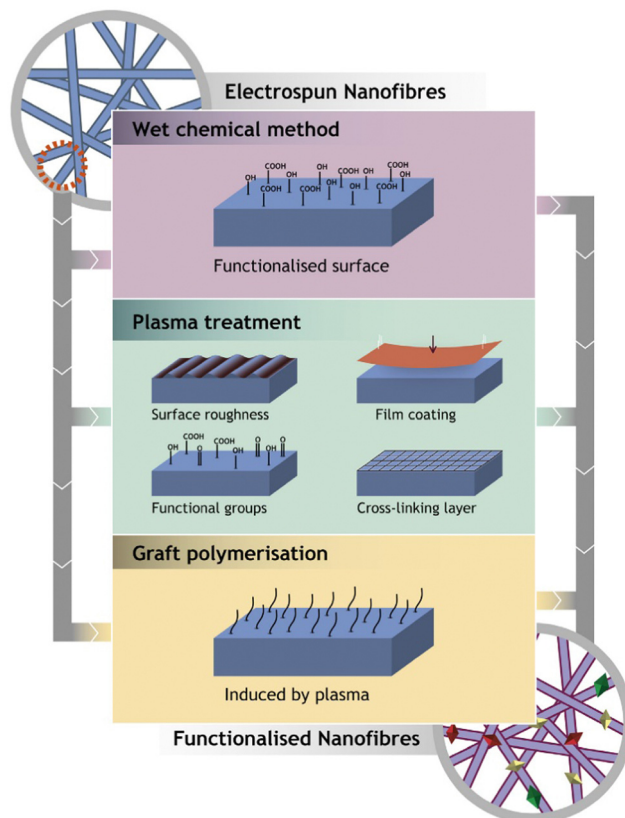Fig. 3 Schematic representation of the electrospinning unit.

Fig. 4 Representation of the main surface modification techniques used to improve the surface nanofibre properties (reproduced with permission from ref. 83 ©2018 Colloids and Surfaces B: Biointerfaces, published by Elsevier Ltd).
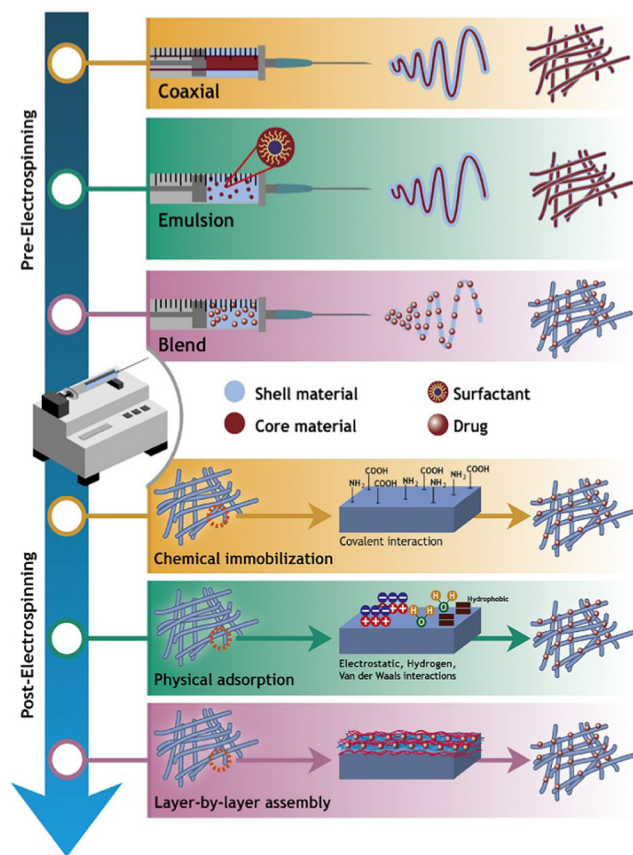
Fig. 5 Illustration of the surface modification techniques used to produce carrier-based drug delivery nanofibres (reproduced with permission from ref. 83 ©2018 *Colloids and Surfaces B: Biointerfaces,* published by Elsevier Ltd).

water.[60] Although reducing pH with acids reduces surface tension, it also has a paradoxical effect on chitosan spinnability since it makes chitosan solutions more viscous. The electrospinning technique enables the fabrication of chitosan nanofibers; however, it encounters various challenges, such as the limited availability of appropriate solvents for the process and numerous factors that impact the quality and yield of the nanofibers. The procedure of electrospinning chitosan is multifaceted due to the unique properties of this polymer in solution, including its polycationic nature, high molecular weight, and the broad range of molecular weights. Several parameters, including molecular weight, solvents, electric field voltage, the inner tip and collector gap, and feed rate, influence the electrospinning process and product quality.[61]

3.1. Influence of the molecular weight

The molecular weight of a polymer indicates the degree of polymer chain entanglement within a solution, a factor that holds considerable importance in the electrospinning process. The molecular weight of chitosan has a notable impact on its electrical properties, including viscosity, dielectric strength, surface tension, and conductivity. Based on a general observation, it was found that an increase in the molecular mass of chitosan resulted in a corresponding increase in the diameter of the fibers.[62] The electrospinning of chitosan with a high molecular weight poses a challenge due to the production of solutions with high viscosity and inadequate chain entanglement. It has been noted that solutions with high molecular weight tend to produce fibers with a larger diameter. In contrast, solutions with a molecular weight that is too low tend to yield beads instead of fibers.[63] Empirical evidence suggests that the impact of deacetylation degree on solution viscosity, and by extension, spinnability, and fiber morphology, is negligible.[64] According to Dogan *et al.*, electrospinning may be feasible with chitosan of light molecular weight, provided that there is macromolecule entanglement.[65] Out of the three chitosan samples tested, only

Table 1 Different types of electrospinning techniques

Electrospinning technique	Bioactive compound	Polymers	Solvent	Results	Ref.
Single nozzle electrospinning	Curcumin	Chitosan PCL Gelatin	Acetic acid HFIP Phosphate buffer saline	Favorable for skin wound dressing Increased fiber hydrophilicity, wettability, and degradability; decreased fiber mechanical properties	Zahiri *et al.* (2020)[84]
Free surface electrospinning	Phycocyanin	*Spirulina* sp. LEB 18 PEO	Acetic acid Water	Enhanced antioxidative activity controlled phycocyanin release	Moreira *et al.* (2019)[85]
Emulsion electrospinning	Catechins	PLGA	Water Chloroform	Controlled release Favorable for skin wound healing Greater antioxidative activity	Ghitescu *et al.* (2018)[86]
Sequential electrospinning	Curcumin	Gelatin Ethyl cellulose	Acetic acid Ethanol Water	Thermally consistent A sustained release lasting 96 hours The antioxidant capacity was maintained	Wang *et al.* (2019)[87]
Uniaxial and coaxial electrospinning	Sour cherry (*Prunus cerasus* L.)	Gelatin Lactalbumin	Acetic acid	Enhanced bio accessibility	Isik *et al.* (2018)[88]
Nozzle-less electrospinning	Thyme	Chitosan Gelatin	Ethanol Acetic acid Deionized water	Antibacterial activity was observed Suitable for nitrite in meat products	Vafania *et al.* (2019)[89]
Coaxial electrospinning	Saffron extract	Zein Tragacanth	Ethanol Water	Regulate saffron release Thermostable Beneficial for diverse culinary uses	Dehcheshmeh and Fathi (2019)[90]
Multi-nozzle electrospinning	Black pepper oleoresin	PCL	Chloroform Butanol	Water-resistance boosted Improved mechanical performance	Figueroa-Lopez *et al.* (2018)[91]

the one with a molecular weight of 106 000 g mol^{-1} and a concentration of approximately 7–7.5% generated a consistent and uninterrupted fiber. The viscosity of this sample ranged from 484 to 590 cP. The electrospun samples obtained from the chitosan solution with lower molecular weight (9.5–10.5%) exhibited a propensity towards the presence of sizable beads and sensitive fibers. In contrast, the specimens derived from the chitosan solution with a higher molecular weight (2.5–3%) exhibited coarser and smoother nanofibers, albeit with some bead defects. The chitosan solution's age must be considered an essential factor in the electrospinning procedure. It is well known that the conformational changes, aggregation, and enzymatic chain scissions in solution may affect the rheological properties of chitosan macromolecules. When utilizing electrospinning, fresh chitosan solutions should be employed to reduce the aging impact.[66]

3.2. Influence of the solvents

The solvent of choice for the electrospinning of nanofibers derived from an aqueous chitosan solution was a concentrated acetic acid solution. Nanofibers exhibiting an average diameter of 40 nm and significant beads were generated initially when the concentration of acetic acid was equivalent to or greater than 30%. The fiber's diameter increased to 130 nm at 90% acid concentration without forming beads. In a 4 kV cm^{-1} electric field, chitosan solutions at 7% concentration in 90% aqueous acetic acid were electrospun to create homogenous nanofiber mats with an average diameter of 130 nm. An important discovery from this study pertained to the substantial influence of acetic acid quantity on the surface tension of chitosan solutions in aqueous environments, particularly in chitosan electrospinning. The surface tension of the liquid decreased from 54.6 dyn cm^{-1} to 31.5 dyn cm^{-1} as the concentration of acetic acid increased from 10% to 90%, while the viscosity remained relatively constant. As the acetic acid content in the water increased, the CS solution's net charge density increased, opening up more charged ions to charge repulsion.[67] The electrospinning process produced orderly CS fibers, utilizing 1,1,1,3,3,3-hexafluoroisopropanol (HFIP) as the solvent. Anisiei *et al.* likely selected HFIP as a solvent in their study "Electrospinning of Chitosan-based Nanofibers" due to its low boiling point of 58 °C and ability to interrupt the solid hydrogen bonding network. This property of HFIP has been previously observed in the electrospinning of other biopolymers. Chitosan solutions were effectively formulated at a concentration of 0.4%, producing amorphous electrospun nanofibers at a mean diameter of 42 ± 15 nm. When utilizing this receipt, it is essential to consider HFIP's volatile and corrosive properties and their potential environmental impact. The observations made during the research point to a minimal concentration of fluoride ions in the fibers, which is roughly two orders of magnitude lower than the World Health Organization's recommended threshold level. Nevertheless, it is essential to acknowledge the challenge of managing substantial quantities of solvent during the electrospinning process. An important discovery from the metal sorption experiment was that the fibers tended to stick together under slightly acidic circumstances (pH = 6); reducing the

active surface area poses a significant disadvantage when the intended application involves a slightly acidic medium.[68] Chitosan in trifluoroacetic acid (TFA) solvent was successfully electrospun, according to research. Chitosan's amino groups and TFA combine to produce salts. This procedure causes an interruption in the rigid interaction among chitosan molecules, rendering them suitable for electrospinning. It is worth noting that while this phenomenon is observed, it is only partially convincing as most acids are known to form salts with chitosan. The significant volatility of TFA presents a favorable characteristic for the rapid solidification of the electrified jet of the chitosan–TFA solution. To enhance the efficiency of the electrospinning process, the addition of dichloromethane (DCM), a volatile solvent, was implemented at varying ratios. Subsequently, the electrospinning process was carried out. The optimal conditions for minimal bead formation in fibers were observed at a solvent ratio of 70 : 30 TFA to dichloromethane (DCM). The resulting chitosan fiber exhibited a mean diameter of 330 nm, with a diameter range spanning from 210 to 650 nm. The morphology of the deposited chitosan was found to be dependent on its concentration in the TFA solution. In SEM images, the coexistence of beads and fibers was observed when the chitosan concentration was 6 wt% or lower. A predominant deposition of fibers was observed at a concentration of 7 weight percent (wt%), while the fraction of beads remarkably decreased. The average diameter was 490 nm, with a diameter distribution ranging from 330 to 610 nm. At a concentration of 8 wt%, the electrospun chitosan fibers exhibited a nearly homogeneous network, with an average diameter of 490 nm and a diameter distribution ranging from 390 to 610 nm.[69]

3.3. Influence of the flow rate

The impact of flow rate on the morphology of the nanofibers is minimal. However, it does affect the electrospinning process. It is necessary to adjust this parameter to promote the formation of the Taylor cone and enhance jet stability. Excessive flow rate results in a solution delivery rate that surpasses the ejection rate of the solution from the tip, leading to the formation of beads at the fiber level. Reduced feed rates are preferred for solvent evaporation and achieving solid nanofibers. The feed rate should be commensurate with the rate at which the solution is removed from the tip. Reduced feeding rates may impede the electrospinning process. In contrast, elevated feeding rates may lead to beaded large-diameter fibers forming due to inadequate solvent evaporation time before reaching the collector. It is advisable to consider the solvent's boiling point when determining the flow rate. The electrospinning process has been shown to emphasize bulk rheological properties at the Taylor cone level. On the contrary, jet thinning amplifies the importance of interfacial properties associated with the concentration gradient and the solvent evaporation rate.[70]

3.4. Electric field effect

The electrospinning procedure is commenced when the electrostatic force in a solution exceeds the surface tension of the said solution. Applying an electric field induces surface charging of

the polymer solution, leading to the acceleration of jet extension, and a complete electrical charge causes the increase in solution volume drawn from the needle. Nevertheless, a high voltage level results in a substantial solution stretch that considerably impacts the morphology of the electrospun fibers, typically resulting in a reduction in fiber diameter and an increase in the likelihood of bead formation.[71]

3.5. Influence of the collector

Another factor affecting nanofibers' sizes and shapes is the separation between their collector and tip. A minimum distance must be maintained to guarantee that the fibers have enough time to dry before entering the collector. Beads have been seen when distances are too near or too vast. This parameter affects the electric field's strength and the jet flight's duration. Reducing the distance between the tip collector has a comparable impact on elevating the voltage. The influence of the collector type on the fiber morphology has been acknowledged. According to previous work,[72,73] the CS/PEO blend solution yielded fibers with smaller diameters and better alignment when collected on a static collector and with bigger diameters and better alignment when collected on a cylindrical spinning collector. It is advised to wind a copper wire to serve as an electrode on the insulation cylinder of the spinning collector to improve the degree of alignment. Simultaneously, the rotational velocity can adjust a specific degree of fiber alignment. Upon reaching a certain velocity, the nanofibers tend to orient themselves, forming mats that combine aligned and misaligned nanofibers. Beyond a particular rotational velocity, the fiber undergoes increased alignment due to mechanical tension and elongation. The mechanical forces exerted also induce a reduction in the fiber diameter.[74] Random deposition of fibers may occur due to excessive drum rotation, which can cause high velocity and instability of the electrified jet. Wang *et al.* claim that the fibers show orientation at velocities greater than 1000 rpm. The separation between the tip of the fiber and the collector influences the shape of the fibers. The variable flight time of the solution between the needle's tip and the collector, which controls the solvent's evaporation time, is linked to this phenomenon. In general, increased distance resulted in decreased nanofiber diameters. However, an excessive distance reduced the electrostatic field, leading to an increase in the diameter of the fiber.[75]

To the best of the authors' knowledge, there is no marketable product of interactive biopolymeric nanofibers on the market, despite the positive potential of these fibrous materials for biomedical applications, which several relevant studies have supported. Due to potential difficulties with large-scale electrospinning of biopolymers, biocompatibility issues resulting from contaminants like cross-linkers and leftover solvents in the fibers, and potentially immunogenic responses brought on by such substances, notably because biopolymer chitosan is rarely water soluble, they must be dissolved in hazardous, very acidic solvents such as 1,1,1,3,3,3-hexafluoro-2-propanol and TFA for electrospinning. Alongside manufacturing, sophisticated testing methods for the generated nanofiber systems must be established and

validated to allow dependable assessment and rapid translation of these devices into clinical applications.[76]

Electrospinning is a potential method for producing submicron fibers, often known as nanofibers, from the laboratory to the industrial level. Many publications have described the synthesis, characterization, and uses of nanofibers. Nanomaterials generally have a high surface area, which benefits applications in several industries. Due to their biocompatibility, adhesion, and sterility, electrospun nanofibers have attracted great interest in the biomedical area,[77–79] applications include filters, protective garments, membranes, sensors, energy storage devices, and catalysis. Nanofibers are now viable for wound dressing materials, scaffold materials, drug delivery systems, filtration membranes, and catalysts for reduction, oxidation, and coupling processes.[80] A few companies have recently presented their work on providing nanofibers for medical devices. Nanofibers are used in batteries and fuel cells as novel materials with higher energy storage capacity. Although the great majority of reported uses are in the biomedical, photocatalytic, and sensor fields, emphasis should be placed on renewable energy storage devices and catalysts for synthesizing organic molecules, medicines, and specialty chemicals.[81,82]

4. Advantages of electrospun chitosan nanofiber platforms

Nanofiber-based systems offer very promising potential as synthetic scaffolds and drug delivery platforms. Nanofibers may provide a suitable matrix for encapsulating and admixing medicinal compounds into a high-efficiency delivery system or reservoir with minimal adverse effects. Furthermore, they could stop medicinal substances from deteriorating before reaching their destinations.[92,93] Nanofiber scaffolds with an architecture
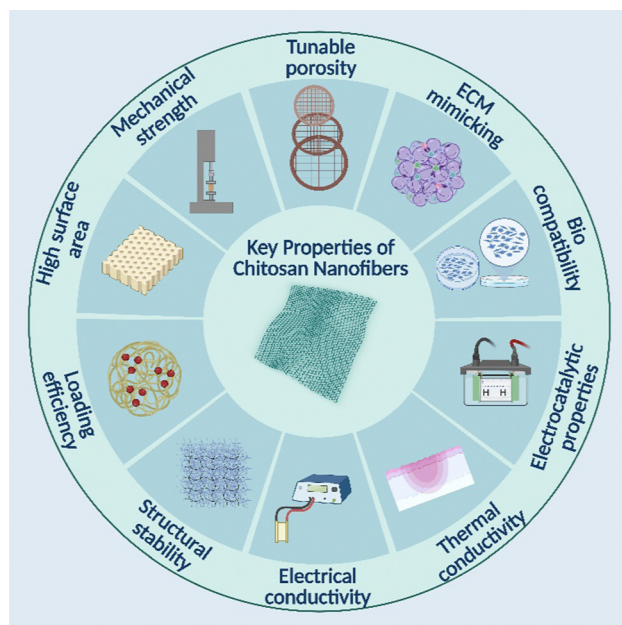

Fig. 6 Key properties of electrospun chitosan nanofibers.

mimicking the natural extracellular matrix (ECM) may provide a large surface area for cell-scaffold contact and adhesion and an adequate exchange for transporting oxygen and nutrients. For tissue-engineered implantation and transplantation, nanofibers may be combined with ECM proteins, growth factors, and nanomaterials to improve the formation of tissue-like structures. As shown in (Fig. 6), chitosan nanofiber mats are an excellent choice for drug delivery because of their numerous advantages and inherent properties. The transport of biomacromolecules, growth factors, small interfering RNA, and antidiabetic pharmaceuticals is one of the most notable characteristics of nanofiber-based structures for biomedical applications.[94] Chitosan-based nanofiber materials for biomedical applications have been created in this area (Table 2).

4.1. Impact of nanofiber beads

The successful preparation of bead-on-string fibers through electrospinning has been achieved by modifying the concentration, charge density, surface tension of the spinning solutions, and electrostatic spinning parameters. The utilization of bead-on-string fibers, which exhibit an alternating distribution of sub-nanofiber and sub-micron beads, has demonstrated significant potential for various applications. The potentially harmful effects of electrospun bead-on-string fibers on the performance of nanomaterials have been considered due to the significant reduction in the surface area caused by the presence of beads, which are usually discarded. In recent times, there has been a surge in interest in them owing to their potential applications in diverse domains such as tissue engineering, drug delivery, and air/water filtration.[95] Subsequent research has demonstrated that incorporating beads in a size range of a few microns is efficacious for drug encapsulation.[96] Spheres can address the issue of incorporating substantial drug dosages in tissue engineering scaffolds, which is otherwise challenging due to the fine nature of electrospun fibers.[97] Bead-on-string fibers have a unique structure that consists of micron-sized spheres and nanometer-sized fibers. This structure creates microporosity that can effectively solve the issues of high air pressure resistance and low filtration efficiency commonly found in highly efficient filtration materials. As a result, these fibers can be utilized in air or water filters to improve their overall effectiveness.[98] Notwithstanding, certain limitations exist, such as the fact that drugs are frequently situated on the fiber surface and cannot be entirely coated, resulting in partial exposure and potential burst release. Hence, the attainment of continuous drug release necessitates the resolution of the issue of sustained drug release. The distribution pattern of sub-nanofiber beads in electrospun bead-on-string fibers exhibits alternating characteristics suitable for fulfilling the requirements of drug loading and sustained release. Larger beads may perform the functions of simple absorption and quick material decomposition to provide drug sustained-release in addition to coating solid particles or water-soluble drugs. Numerous researchers have extensively studied the role of electrospun bead-on-string fibers in sustained drug release. Somvipart et al. demonstrated that sustained drug release could be achieved using bead-on-string fibers. The experiment aimed to compare the release effects of smooth electrospinning fibers and bead-on-string fibers with the same amount of drug loading within a 120 hour timeframe. According to the results, the smooth nanofibers exhibited a drug release rate of up to 80% within 10 hours. Additionally, there was a significant occurrence of burst drug release. Upon loading the drug onto the bead-on-string fibers, it was observed that the release amount of the drug was less than 50%, suggesting that using bead-on-string fibers as a drug carrier can improve the issue of burst release from smooth fibers, leading to better control and sustained release of the drug.[99] In their study, Wang et al. examined the filtration process of bead-on-string fibers and discovered that the presence of beads can significantly enhance the effectiveness of air filtration. The membranes possess promising characteristics that make them suitable for filters in various applications such as indoor air purification, respiratory protection, and other filtration applications.[100] Yun et al. studied the filtration properties of fiber mats with varying morphologies. They achieved this by creating bead-on-string fiber mats and particle/nanofiber composites. According to the results, the durability factor for the composite fiber mat and bead-on-string fiber mat was superior to that of the nanofiber mats.[101] In summary, bead-on-string fibers exhibit potential utility in various domains such as drug delivery, tissue engineering, water, and air filtration.

4.2. Impact of nanofiber porosity

The presence of porosity in nanofiber scaffolds is a crucial aspect as it enables cells to reach the accessible surfaces of the fibers. Due to the lack of porosity, access to these surfaces would be impeded. Furthermore, the pores within the nanofiber scaffold must be interconnected to facilitate cellular migration. Failure to do so may result in restricted cell proliferation confined to the surface of the nanofiber mat, which reduces the effective surface area available for cellular growth on the scaffold. The oxygen permeability of nanofibers is facilitated by their porosity, which in turn fosters the development of a microenvironment conducive to tissue regeneration. The assessment of porosity in a nanofiber scaffold is frequently conducted using mercury porosimetry, a technique that involves the application of high pressures to force mercury through the scaffold.[102] This method yields data about the total pore volume and the pore size. According to published reports, electrospinning techniques have been employed to produce CS and other polymer nanofibers under various circumstances. The nanofibers possess essential features involving the ability to mimic the extracellular matrix (ECM), biocompatibility, and regulated biodegradability. Also, the lower water contents of the PVA and the higher surface amine group of the CS both impacted fiber diameter and could stimulate cell adhesion, proliferation, and differentiation.[103] These nanofibers' enhanced properties are vital for their application in tissue engineering. Numerous studies have been conducted to produce chitosan/nBGC hybrid scaffolds through the lyophilization method. In addition to their capacity to become bioactive, the nanocomposite scaffolds have shown appropriate swelling and degradation characteristics.[104] The porosity of the composite scaffolds was deemed satisfactory upon achieving a homogeneous

Table 2 A summary of available chitosan-based nanofiber materials for biomedical application

S. no.	Nanofiber material	Key features	Biomedical application	Ref.
1	CS–PCL nanofibers	Promoted complete wound healing and closure	Skin tissue engineering	Levengood et al. (2018)[155]
2	CS–gelatin–PCL nanofibrous scaffold	Possess suitable physical, chemical, and biological characteristics	Skin tissue engineering	Gomes et al.(2017)[156]
3	CS–vitamin C–lactic acid composite membrane	Increased NIH 3T3 cell attachment, growth, and proliferation	Skin tissue engineering	Madni et al.(2019)[157]
4	CS–PCL blend fibrous mat	Improved tensile strength, thermal stability, surface roughness, and swelling properties. Enhanced attachment and proliferation of keratinocytes	Skin tissue engineering	Prasad et al.(2015)[158]
5	Collagen–CS scaffolds	Accelerates cell proliferation	Skin tissue engineering	Tangsadthakun et al. (2017)[159]
6	Gelatin–CS electrospun scaffold	92% porosity. Good tensile strength. Displaying a spindle-like shape	Skin tissue engineering	Pezeshki-Modaress et al. (2018)[160]
7	CS–PCL nanofibers	Appropriate cell attachment, viability, and metabolic activity	Bone tissue engineering	Jing et al.(2015)[161]
8	CS-clay-hydroxyapatite scaffold	Enhanced mechanical and biological properties	Bone tissue engineering	Kar et al.(2016)[162]
9	Strontium hydroxyapatite–CS nanohybrid scaffolds	Demonstrates outstanding osteoinductivity	Bone tissue engineering	Lei et al. (2017)[163]
10	CS anchored on porous PCL-bioactive glass composite scaffolds	Improved cell adhesion, osteogenic differentiation, and protein adsorption. Encouraged the regeneration of cranial bones	Bone tissue engineering	Li et al.(2019)[164]
11	CS–PLA scaffolds using different cross-linkers	Improved physical properties. Encourage chondrogenesis	Cartilage tissue engineering	Mallick et al. (2016)[165]
12	PHB-CS blend fibrous scaffolds	Increased adhesion of chondrocytes	Cartilage tissue engineering	Sadeghi et al. (2016)[166]
13	SF-CS porous scaffold	Improved cell adhesion viability and proliferation	Cartilage tissue engineering	Vishwanath et al. (2016)[167]
14	CS–PLA–pectin composite scaffolds	Superior neo-cartilage tissue regeneration. Demonstrates appropriate swelling properties. Moderate biodegradation and hemocompatibility profile. Necessary mechanical strength	Cartilage tissue engineering	Mallick et al. (2018)[168]
15	CS–collagen/hydroxyapatite scaffold	Inexpensive materials. Poor mechanical properties	Cartilage tissue engineering	Kaviani et al. (2019)[169]
16	Glycosaminoglycans–CS complex membranes	Removes incomplete endothelialization. Smooth muscle cell hyperplasia to address the shortcomings of existing small-diameter vascular grafts	Blood vessel tissue engineering	Chupa et al. (2000)[170]
17	CS-derived sandwiched tubular scaffold	Pore diameter control. Extremely high burst strength. Strong suture retention	Blood vessel tissue engineering	Zhang et al. (2006)[171]
18	Collagen–CS–thermoplastic PU nanofibrous scaffold	High tensile strength and flexibility. Uncertainty regarding in vivo plastic degradation	Blood vessel tissue engineering	Huang et al. (2011)[172]
19	CS–PCL nanofibrous scaffold	Being characterized by anticoagulant. Quickly re-endothelializing properties	Blood vessel tissue engineering	Du et al. (2012)[173]
20	CS/gelatin bi-layer microporous scaffold	Similar morphological and mechanical characteristics to blood vessels; tubular architecture	Blood vessel tissue engineering	Badhe et al. (2017)[174]
21	Chitosan-HAp scaffolds loaded with basic fibroblast growth factor	Better cellular organization, proliferation, and mineralization	Periodontal tissue engineering	Akman et al. (2010)[175]
22	Chitosan-bioactive glass nanoparticles composite membranes	Increases bioactivity properties. Favorable for periodontal regeneration	Periodontal tissue engineering	Mota et al. (2012)[175]
23	PLA and CS–PLA blends nanofibrous scaffolds	BMSCs' osteogenic differentiation and cell adhesion were enhanced; human periodontal ligament cells' expression of inflammatory mediators and TLR4 (Toll-like receptor 4) was increased.	Periodontal tissue engineering	Shen et al. (2018)[176]
24	Hydroxypropyl CS–gelatin scaffold	Increased cell compatibility and surface growth of Keratocytes	Corneal regeneration	Wang et al. (2009)[177]
25	Hydroxyethyl CS–gelatin and chondroitin sulfate blend scaffold	Transplant corneal endothelial cells its water content, ion permeability, and glucose permeability were strikingly similar to the natural cornea	Corneal regeneration	Liang et al. (2011)[178]
26	CS–SF scaffold	Comparable lamellar cornea reconstruction	Corneal regeneration	Guan et al. (2013)[179]
27	Chitosan–PCL blend	Limited biodegradability. Sufficient alternative to cadaveric corneal transplantation	Corneal regeneration	Wang et al. (2019)[180]
28	CS/cellulose nanofibers	Intervertebral disc regeneration. Preventing mechanical disc failure	Intervertebral disc tissue engineering	Doench et al. (2018)[181]

© 2023 The Author(s). Published by the Royal Society of Chemistry

Table 2 (continued)

S. no.	Nanofiber material	Key features	Biomedical application	Ref.
29	CS-based hydrogels, filled with cellulose nanofibers	Regenerated the IVD and AF tissue of the intervertebral disc	Intervertebral disc tissue engineering	Doench et al. (2019)[182]
30	CS hydrogel/poly (butylene succinate-co-terephthalate) copolyester electrospun fibers	Increased mechanical properties. A promising candidate for IVD replacement therapies	Intervertebral disc tissue engineering	Yuan et al. (2019)[183]
31	Chitin fiber and chitosan composites	Improved thermal stability and crystallinity. Insufficient bending modulus and strength. Potential bone fractures	Tissue fixation	Wang et al. (2010)[184]
32	Chitosan and nanocrystalline hydroxyapatite composites	Improved cellular behavior. Increased mechanical strength and cell compatibility	Tissue fixation	Pu et al. (2012)[185]
33	Oxidized dextran and CS-based surgical adhesives	Effectively binds tissues. Stops bleeding. Possesses tissue-sealing properties. Serves as a hemostat. The delivery of drugs, peptides, and proteins	Tissue fixation	Balakrishnan et al. (2017)[186]

distribution of bioactive glass-ceramic nanoparticles (nBGC) across the pore walls. Several reports on using chitosan alone or in conjunction with other polymers indicate that these biopolymers have enormous potential for tissue engineering and may be tailored to meet the growing demands of this field. The chitosan membrane modified with arginine and electrospun exhibits a complete porosity of $88.25 \pm 4.13\%$, which falls within the desired 60–90% range. The advantageous attribute of these systems lies in their porous nature, which facilitates cellular infiltration and proliferation. In addition, porosity is crucial in facilitating the appropriate exchange of gases, nutrients, and fluids, which are critical factors in achieving hemostasis and ultimately enabling optimal wound healing.[105]

4.3. Swelling profile of chitosan nanofibers

The utilization of pure chitosan nanofibers in tissue engineering may be limited due to their mechanical instability and uncontrollable swelling. Chitosan nanofibers absorb moisture and swell when exposed to aqueous and physiological environments, which can lead to a loss of stability in the fibrous structures and insufficient mechanical properties. Over the last few decades, the wet stability of electrospun chitosan-based nanofibers has been improved through different crosslinking methods, such as physical, chemical, and ionic crosslinking. Several crosslinking methods have been employed to enhance the wetting resistance and stability of chitosan-based nanofibers produced through electrospinning. Chitosan's amine group can be crosslinked using various crosslinkers such as glutaraldehyde, epichlorohydrin, and genipine. Chitosan nanofibers can be chemically crosslinked to form permanent crosslinking networks through chemical reactions between chemical crosslinkers and the functional groups of the chitosan chain.[106,107] Genipine has been utilized as a biocompatible crosslinker to address the cytotoxicity drawbacks commonly associated with glutaraldehyde. Studies have shown that glutaraldehyde can crosslink chitosan through Schiff base formation. While glutaraldehyde has been found to enhance the wet stability of chitosan-based nanofibers, several reports have indicated that using glutaraldehyde in crosslinking these materials can result in cytotoxicity.[108] Physical forces

such as hydrogen bonds, polar bonding, electrostatic contact, and van der Waals interactions between molecular chains were primarily used to create physically crosslinked chitosan nanofibers. In comparison to chemical crosslinkers, ionic crosslinkers provide the advantages of reduced toxicity and decreased environmental pollution.[109,110] The ionic crosslinking process may also coincide with supplementary interchain interactions such as hydrogen bonding, which involve the hydroxyl groups of chitosan and the ionic molecules. The utilization of chitosan-based functional nanofibers has emerged as a novel trend in their development. Kiechel et al. explored the application of TPP and TA as non-covalent crosslinkers for chitosan fibers produced through electrospinning. Chitosan's cationic amino groups can create ionic interactions with negatively charged molecules and anions. Small anionic molecules such as sodium tripolyphosphate (TPP), tannic acid (TA), and glycerol phosphate are frequently used to crosslink chitosan nanofibers. In their study,[111] whether it was utilized for heating or base activation, the crosslinking process was carried out either before or after electrospinning with TA, employing a one-step or two-step method to prevent immediate crosslinking during electrospinning and avoid clogging the syringe and needle; TPP crosslinking was carried out in two stages, with the option of heat or base activation. According to the conclusions, the two-step chitosan–TA was completely crosslinked and remained intact even after 72 hours in 1 M acetic acid (pH 3). In contrast, the chitosan–TPP and active two-step chitosan–TA fibers were only partially crosslinked and could withstand water (pH 6) for 72 hours.[112] Wang and their colleagues utilized a combination of electrospinning and subsequent lyophilization to create fibrous hydrogels based on chitosan. By incorporating 30% cellulose acetate nanofibers, the cellular structure of the hydrogel could be maintained in water without the need for chemical crosslinking. Furthermore, including 60% of these nanofibers ensured that the chitosan hydrogel maintained its freestanding structure, even with a low solid content of only 1%.[113] The application of butyric acid modification to chitosan nanofibers resulted in the formation of butyroylated chitosan nanofibers (BCSNF), which exhibited a significant reduction in swelling by 75% and an increase in mechanical strength by nearly double.[114] Furthermore,

sulfonated chitosan was synthesized by treating chitosan with chlorosulfonic acid. The resultant composite scaffolds comprising sulfonated chitosan and PCL nanofibers significantly enhanced the mechanical properties.[115]

4.4. Biodegradation

The principle of degradation of polymer-based materials depends on surface erosion if a catalytic substrate or molecules are present in the degradation medium or environment. Chitosan degradation is an essential topic in the biomaterials field, and researchers were keen to discover more about the chitosan molecule's degradation behavior. The transition from bulk deterioration to surface erosion is determined by measuring material thickness. It is significant to highlight that the erosion process resulting from hydrolytic degradation is contingent upon the structural composition of the material.[116] Most biodegradable polymers undergo degradation *via* a bulk erosion mechanism without catalytic molecules. Conversely, the ions exert their influence solely on the material's surface rather than undergoing diffusion into the interior, resulting in erosion of the chitosan surface while the core stays unaltered. Various techniques have been employed in chitosan degradation engineering to produce chitosan that exhibits degradation kinetics ranging from days to months, contingent upon the specific application of the device. This process's regulation can be achieved by carefully selecting the optimal molecular weight and deacetylation degree. Nazrul *et al.* observed a connection between the rate of degradation and molecular mass, the distribution of *N*-acetyl D-glucosamine residues, the degree of deacetylation, and, subsequently, crystallinity.[117] The rate of biodegradation is positively correlated with the reduction in crystallinity. Chitosan chains with lower molecular weight exhibit greater biodegradability than those with higher molecular weight. Furthermore, in the case of certain polyelectrolyte complexes with weak associations or hydrogels with minimal crosslinking, the degradation process may be significantly influenced by non-enzymatic hydrolysis, wherein the breaking of electrostatic interactions or cleavage of crosslinker molecules by water may occur. The larger implants may experience acid-mediated hydrolysis at their surface, which can be attributed to the acidic conditions generated by macrophages that remain activated over a prolonged period.[118] Chitosan was noticed to undergo *in vivo* degradation *via* a range of non-specific enzymes, with particular emphasis on lysozyme, which is ubiquitously present in mammalian tissues. Chitosan degradation *in vitro* can occur through oxidation, chemical hydrolysis, or enzymatic hydrolysis. The process of chitosan biodegradation results in the liberation of monosaccharides, which can be assimilated into the metabolic pathways of glycosaminoglycan and glycoprotein or eliminated from the system. The enzymatic hydrolytic degradation of chitosan in the human body is primarily attributed to lysozymes and can be effectively simulated through *in vitro* analysis. The degradation of chitosan by lysozymes occurs through the cleavage of glycosidic linkages between the polysaccharide units within the polymer. This procedure yields glucosamine and saccharide, which can either undergo metabolic processes or be stored as proteoglycans within the human body.[119] Cracking, swelling, and

dissolving are physical degrading processes for chitosan implants, while oxidation, depolymerization, and hydrolysis (enzymatic or non-enzymatic) are chemical processes. Chitosan products with low molecular weight, oligosaccharides, and functionalization can potentially be water-soluble and consequently more prone to simple hydrolysis.[120] These mechanisms may be modeled both *in vivo* and *in vitro*. Non-enzymatic hydrolytic processes only play a limited role in the breakdown of highly crystalline types of chitosan due to the slow-rate hydrolytic destruction of glycosidic linkages between the polysaccharide units.[121] Sarhan *et al.* conducted a study wherein they synthesized a composite nanofiber consisting of CS, PVA, and honey. The study's findings revealed that the nanofibers' degradation decreased upon crosslinking with CS, PVA, and honey compared to the non-cross-linked nanofibers.[122] The Yu *et al.* cohort researchers employed physical adsorption techniques to coat the chitosan nanofibers' surface with hydroxyapatite and collagen. The application of this coating facilitates the utilization of this composite nanofiber as a structure for regulated degradation over an extended duration.[123] Liu *et al.* created a wound dressing material comprising a bi-layer composite. The upper layer of the composite was composed of soybean protein non-woven fabric, while the lower layer was coated with genii crosslinked chitosan film. The composite was tested in a rat model to investigate the effects of wound treatment *in vivo*. The experiment results indicate that the genipin content can be controlled to regulate the degree of crosslinking and the *in vitro* degradation rate of the chitosan films crosslinked with genipin.[124] The rate of degradation of scaffolds is a crucial parameter for bone regeneration as it creates interstitial spaces within the tissue, thereby facilitating matrix deposition, as has been reported in the literature. The *N*-acetyl glucosamine (NAG) moiety present in the structure of chitosan is susceptible to degradation by lysozyme, which serves as a key enzyme responsible for the degradation of chitosan chains.[125] Chitinases, enzymes specifically targeting chitosan or chitin, can be detected in limited quantities within the human body. Examples of such chitinases include chitotrioqasidase and acidic mammalian chitinase (AMCase).[126] Certain organ systems, especially the colon, and intestines, may harbor bacterial flora that produce digestive enzymes, including β-glucosidase. This enzyme is responsible for the depolymerization and degradation of chitosan.[127] The potential impact of bacterial degradation is a significant factor to consider in drug delivery systems aiming to target intestinal glucosidase or other digestive tract segments. Furthermore, tissue damage and active infection caused by bacteria or fungal pathogens may result in unfavorable degradation. A study was conducted by Su *et al.* to investigate the *in vivo* degradation of carboxymethyl chitosan (CMCS) at a concentration of 20% weight by weight. The hydrogel was administered intradermally into the dorsal region of the rodents at ambient temperature. A significant proportion of the administered gels exhibited a rapid degradation rate, with the majority undergoing complete disappearance within 10 days post-injection. The CMCS hydrogels underwent complete degradation and resorption within 19 days.[128] Chitosan's biocompatibility and ability to degrade in a controlled manner render it an appropriate choice for utilization as a membrane barrier in the

guided bone regeneration (GBR) context. The GBR technique is employed as a surgical intervention to preserve the space at the site of periodontal bone defects. The high degradation rate of chitosan as a standalone polymer poses a significant constraint in its application for tissue engineering purposes.[129]

4.5. Modification of chitosan using amino acids

Chitosan exhibits remarkable properties among the diverse polymers employed in producing nanofibers. The field of chitosan has demonstrated the capacity to impede the proliferation of certain bacterial strains. Infected wounds can impede the healing process to a significant extent and, in certain instances, even hinder it. The potential therapeutic application of chitosan is attributed to its desirable bacteriostatic activity. The observed antimicrobial activity could be attributed to the interaction between the amino groups, which carry a positive charge, and the negatively charged groups on the surface of bacterial cells. This phenomenon results in the disruption of microbial membranes, leading to the release of intracellular constituents such as proteins.[130] Notwithstanding its inherent activity, the antimicrobial efficacy of chitosan can be enhanced through augmentation of the cationic moieties on its backbone. Several modifications have been implemented to enhance the antibacterial properties of chitosan. The current focus is on amino acids, the fundamental building blocks of proteins, and their potential as antibacterial agents when combined with chitosan. The task above can be achieved by grafting amino acids with a positive charge, namely L-asparagine, L-arginine, or L-lysine. Including L-arginine is anticipated to augment the count of cationic groups at physiological pH, primarily owing to the presence of the guanidine moiety ($pK_a = 12.5$). The anticipated outcome of this incorporation is the augmentation of the antibacterial characteristics of chitosan. In addition to the phenomenon of charge delocalization among the three nitrogen atoms in the arginine molecule, the antimicrobial properties of these amino acids can also be attributed to their electrostatic interactions with the bacterial membrane. The current investigation pertains to the generation of electrospun fibers comprising L-arginine-modified chitosan and deacetylated chitosan through the utilization of 1-(3-dimethylaminopropyl)-3-ethylcarbodiimide hydrochloride and N-hydroxy succinimide.[131] The generated fibers are intended to be employed as a membrane for a wound dressing. The NH_2 groups of chitosan with the COOH of arginine were successfully combined to create a peptide bond during the preparation of the membranes utilizing the freeze-drying method. The amide I peak observed at approximately 1654 cm^{-1} in chitosan–arginine can be deduced from the results of the FTIR analysis. This finding offers substantiation for the conjugation of arginine to the chitosan structure *via* a grafting linkage. A significant reduction in bacterial growth, amounting to 99.99%, was noted in the antibacterial activity produced by *E. coli* and *S. aureus*.[132]

4.6. Silver nanoparticles loaded with nanofibers

Scaffolds within the nanoscale range have garnered significant interest due to their appealing characteristics, such as their ability to transport bioactive agents, elevated surface area,

enhanced mechanical properties, emulation of the extracellular matrix, and substantial porosity.[133] Chitosan nanofibrous materials have the potential to be encapsulated or loaded with metal-based nanoparticles, which can augment their therapeutic efficacy in wound healing applications. Metal-based nanoparticles, specifically silver nanoparticles, have been extensively researched and have demonstrated favorable characteristics, including exceptional antibacterial activity, antioxidant and anti-inflammatory properties, and promotion of cell growth. These attributes make them a crucial bioactive component in wound dressings. Hybrid materials consisting of chitosan and silver nanoparticles (AgNPs) are of significant interest due to their antibacterial characteristics, rendering them a promising option for fabricating wound healing devices. The antimicrobial activity spectrum of the nanosilver films showed great potential.[134] Hybrid systems comprising chitosan–AgNPs require high surface area-to-volume and aspect ratios to demonstrate antimicrobial activity. The previously mentioned characteristics promote efficacious interaction between the hybrid substance and the cellular membranes of highly pathogenic microorganisms, thereby leading to biocidal efficacy.[135] Nanofiber mats were produced *via* electrospinning techniques utilizing carboxyethyl chitosan (CEC) and AgNPs. CEC has functional groups with amino and carboxylic acids that may chelate silver ions. $AgNO_3$ was converted into AgNPs under favorable conditions by electrospinning with concentrated formic acid as the solvent. Two primary methods were utilized to produce insoluble nanofibers containing silver ions. These techniques include reactive electrospinning, a one-step procedure, and cross-linking the non-woven fabric with GA vapors after electrospinning, a two-step procedure. Scanning electron microscopy was used to analyze the morphology of the fibers. Energy-dispersive X-ray spectroscopy was used to assess the arrangement of AgNPs in the nanofibers' structure. The quantification of the content present on the fiber's surface was ascertained *via* X-ray photoelectron spectroscopy.[136]

The fibers may significantly delay the medication release in liposomes. For instance, gentamicin-loaded maleimide liposomes were grafted on the surface of CS fibers by covalent processes after Monteiro *et al.* treated the surface of the fibers with various thiolation chemicals. According to *in vitro* tests, *E. coli*, *P. aeruginosa*, and *S. aureus* are all susceptible to the antibacterial activity of gentamicin released from liposomes immobilized at the surface of electrospun fibers. Since these pathogens are a frequent source of local infections, our findings indicate that the proposed nanostructured delivery method has promise for wound management applications. It may also be employed to eradicate these pathogens.[137,138]

Chemical modification has also been applied to improve the solubility and spinnability of chitosan. Chemically altered chitosan derivatives include hexanoyl chitosan,[139] PEGylated chitosan,[140] carboxyethyl chitosan,[141] and quaternized chitosan.[142] Because of this, chitosan derivatives are soluble in acidic, neutral, and essential aqueous solutions.[143] Chitosan's water solubility, for instance, may be significantly improved by adding carboxymethyl to the molecule.[144] The most straightforward technique to increase chitosan's spinnability is combining it with another natural or

synthetic polymer. Collagen,[145] gelatin,[146] cellulose,[147] PEO,[148] PVA,[149,150] PCL,[151,152] and poly(lactide-*co*-glycolide) are among the co-spinning agents that have been extensively studied by research teams throughout the globe.[153,154] An area of materials research that is fast expanding is the use of nanofibers in the conception and creation of novel products. This study concentrates on the most recent advancements in chitosan-based nanofibers, their derivatives, blends, and composites to highlight natural polymers' future significance and potential usage in intelligent materials. This article discusses the difficulties, patterns, and possible uses of nanofibers made from chitosan for biomedical purposes.

5. Biomedical application of electrospun chitosan nanofibers

The development of novel scientific theories and the effective addressing of environmental and social issues, particularly in large-scale material manufacturing, are necessary for sustainable nanotechnology's future. The most significant obstacles in this regard are those related to producing goods based on nanoscales while maximizing the use of "green" materials (regarding the chemistry involved). Natural biopolymers often exhibit superior biocompatibility to synthetic materials, which makes them better suited for usage in the human body. In various biomedical and pharmacological applications, such as tissue engineering, surgical devices, and body-implant interphases, electrospun fibers of these biomaterials may be of significant interest. As mentioned previously, electrospun available chitosan nanofibers offer enormous promise for various biological uses. Essential qualities are necessary to design and produce nanofibers for particular applications and practical usefulness. They may be attained by factors linked to the method,

Fig. 7 A diagrammatic illustration of the biomedical applications of electrospun chitosan nanofibers.

composition, and surrounding ambient conditions.[187] The biocompatibility and biomechanical qualities of the nanofibers and scaffolds are increased, which improves their performance. The biomedical uses of electrospun chitosan nanofibers and scaffolds are thoroughly covered in this section.[188] Potential areas for electrospun chitosan nanofiber use in the biomedical field are shown in Fig. 7.

5.1. Wound dressings

CS is an excellent substance for creating these antimicrobial dressings since they have a well-known wound-healing tendency (Table 4). Additionally, nanofibers' structures are like those of the skin's ECM, which speeds up the process of healing.[189] CS was discovered to activate macrophages and hasten the healing of wounds. Additionally, CS promotes the migration of polymorphonuclear neutrophils during the beginning of the wound healing process, granulation tissue development, and collagen production by fibroblasts (Table 3). CS has also been shown to help re-epithelialize and rejuvenate the granular layer of skin.[190] Ardila *et al.* demonstrated two distinct methods for producing nonwoven mats comprising CS and bacterial nanocellulose using the electrospinning process.[191] The first method involved electrospinning CS and bacterial nanocellulose solutions simultaneously through two syringes aimed at the same target. The second method used coaxial electrospinning to create core–shell structures by electrospinning bacterial nanocellulose and CS simultaneously through a spinneret made of two concentric needles. In both methods, co-spinning agents were necessary. Due to the incompatibility of their respective solvents, a direct mixture of CS and bacterial nanocellulose and consequent electrospinning was not practical. The first method made creating mats comprising CS and bacterial nanocellulose nanofibers possible. Nevertheless, a few bacterial nanocellulose threads were in the collection to enhance fiber production and assembly; they introduced a co-spinning agent, polylactide, and raised the solution temperature between 22 and 60 °C during the electrospinning process. However, the most significant outcomes for manufacturing nanofibers comprising chitosan and bacterial nanocellulose came through coaxial electrospinning. Aqueous CS–PEO solutions were used to create high yields of nanofibers, with bacterial nanocellulose solutions serving as the outer layer. Finally, a 99.9% reduction in the population of *E. coli* was observed in the mats made using the coaxial technique *versus* the control. They proposed that this was most likely caused by the ionic interaction between the positively charged amino groups and the bacteria's negative surface charge, which decreased membrane permeability, cell leakage, and eventual death.

Zhou *et al.* in 2017 created bi-component nanofiber scaffolds of photo-crosslinked maleiled CS–methacrylate polyvinyl alcohol (MCS-MPVA) with improved water stability by electrospinning an aqueous MCS-MPVA solution and subsequent photopolymerization. According to the results of a water stability test, the photocrosslinked matrix with a 10 : 90 ratio of MCS-MPVA maintained the exceptional integrity of the fibrous structure. The photocrosslinked nanofiber scaffolds showed excellent cellular compatibility and might be employed as a
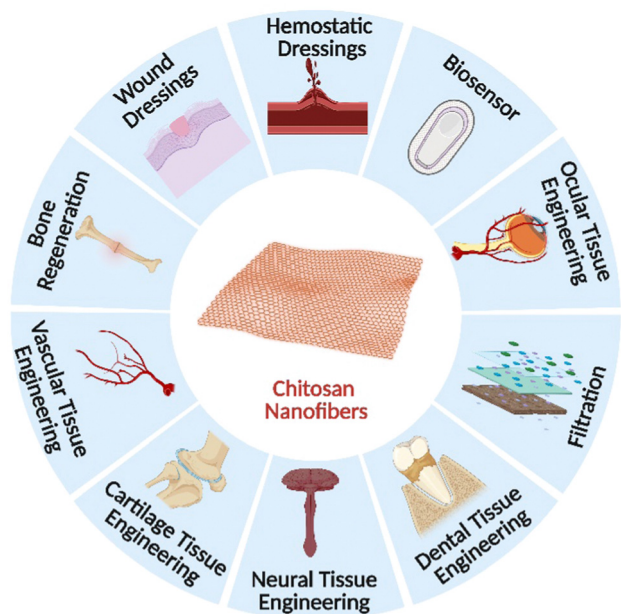
Table 3 Chitosan electrospun nanofibers for wound dressing application

Chitosan nanofiber biomaterials	Electrospinning technique	Solvents	kV	cm	mL h^{-1}	Diameter (nm)	Target microbe	Target Cell line	Ref.
Curcumin, CS, PCL	Single nozzle	DCM DMF	21	12	0.5	99.84	MRSA E. coli	HDF	Fahimirad et al. (2021)[195]
Quercetin, CS, PCL	Single nozzle	AcOH HCOOH	3	15	0.77	119.1 ± 24.6	S. aureus E. coli	NIH3T3	Zhou et al. (2021)[196]
Mupirocin, CS, PCL	Single nozzle	HFIP DCM	15	15	1	440–1580	S. aureus E. coli	HDF	Li et al. (2018)[197]
Garcinia mangostana CS, EDTA, PVA	Single nozzle	H$_2$O	15	20	0.25	205–251	S. aureus E. coli	NHF	Charernsriwilaiwat et al. (2013)[198]
Eugenol, CS, PVA, PCL	Emulsion	CHCl$_3$ DMF AcOH	75	13	—	379.05	S. aureus P. aeruginosa	HDF	Mouro et al. (2016)[199]
Henna leaves extract CS, PEO	Single nozzle	AcOH	5–25	10–20	0.1–1.5	64–89	S. aureus E. coli	NHF	Yousefi et al. (2017)[200]
Zataria multiflora oil, CS, PVA, gelatin	Single nozzle	AcOH H$_2$O	21	15	0.2	218 ± 58	S. aureus P. aeruginosa	L929	Ardekani et al. (2019)[201]
Ciprofloxacin, CS, PEO, silica	Single nozzle	AcOH	8–12	11–13	0.5	472 ± 70	S. aureus E. coli	L929 HFFF2	Kataria et al. (2014)[202]
Tetracycline HCl, CS, PVA, sericin	Single nozzle	AcOH	15	20	2.50	305–425	E. coli S. aureus	L929	Bakhsheshi-Rad et al. (2020)[203]
Cefadroxil monohydrate, CS, PVA	Single nozzle	AcOH H$_2$O	30	14	1	290 ± 86	S. aureus	HaCaT	Iqbal et al. (2020)[204]
ZnO, CS, PVA	Single nozzle	AcOH H$_2$O	—	7	0.5	891.72	B. subtilis E. coli		Ahmed et al. (2018)[205]
ZnONPs, collagen, CS	Single nozzle	AcOH	15	12	0.3	—	S. aureus E. coli	HDF	Sun et al. (2019)[206]
Deacetylated/arginine-modified CS	Single nozzle	TFA DCM	28	10	1.2	492	E. coli S. aureus	HDF	Antunes et al. (2015)[207]
CS–SF nanofibers	Single nozzle	HFIP	20	12–15	0.8	185.5 ± 114.7	E. coli S. aureus	MEF	Cai et al. (2010)[208]
CS–sericin nanofibers	Single nozzle	TFA	18	15		380	E. coli B. subtilis	L929	Zhao et al. (2014)[209]
CS–PCL nanofibers	Coaxial	DCM Ethanol	25	10–12	0.2 & 0.4	240 ± 50	—	HaCaT	Poornima and Korrapati (2017)[210]
Graphene oxide-modified CS/PVP nanofiber	Single nozzle	AcOH water	24	13	0.3	60	E. coli P. aeruginosa S. aureus	MSCs	Mahmoudi and Simchi (2017)[211]
CS–PEO/fibrinogen biocomposite nanofiber	Dual-spinneret	AcOH BSA DMSO	28	22	1.0	351.1 ± 101.7	E. coli S. aureus	HDF	Yuan et al. (2018)[212]
Oleoyl–CS-based nanofibers	Single nozzle	AcOH	20–22	15–18	2 µL min^{-1}	150–400	—	hAMCs	Datta et al. (2017)[213]
Hydroxypropyl trimethyl ammonium chloride chitosan functionalized-PLGA	Single nozzle	HFIP	12	15–20	1.5–2.0	450	S. aureus P. aeruginosa	HDF HaCaT	Yang et al. (2017)[214]
CS/PCL–hyaluronic acid bilayered scaffold	Single nozzle	HCOOH Acetone	16	15	1.2	362.2 ± 236	E. coli	Vero cells	Chanda et al. (2018)[215]

wound dressing, according to an investigation of their cytotoxicity on L929 cells.[192] For use in wound dressings, Alavarse et al. formulated two electrospun mats, including PVA–CS and PVA–CS/tetracycline hydrochloride (TCH). They also looked at their cytotoxicity, drug release, antibacterial, thermal, morphological, mechanical, and other qualities. The results showed no significant changes in the thermal and morphological characteristics of the mats and integrated the drug evenly along the nanofibers. The drug release profile within the first two hours revealed a burst delivery, demonstrating significant antibacterial action on E. coli and S. aureus, and S. epidermidis. The generated drug-loaded nanofiber scaffolds showed high cytocompatibility in an indirect, in vitro MTT experiment. A scratch assay further supported this, suggesting that the scaffold may be employed as an antibacterial dressing for healing.

Many compounds have been included within their structures to boost their antibacterial capabilities. Synthetic/natural antibiotics, metal nanoparticles, and vitamins have essentially been the principal components of such antimicrobial agents. An example of a polymeric antimicrobial covering facilitates the movement and transformation of fibroblasts and functions as a physical barrier to prevent microorganisms from entering the wound. Due to the open wound's susceptibility to bacterial contamination, the inflammatory phase is prolonged, and the production of metalloproteinases is elevated. These metalloproteinases prevent new granulation tissue growth while degrading ECM components. The antimicrobial dressing is a physical barrier to block the entry of infections into the wound and kills invasive germs by covering the wound bed. The antimicrobial coating also promotes the immune system, fibroblast, and keratinocyte migration, which aids in the healing process.[193] Etterami et al. coated insulin-delivery CS nanoparticles onto electrospun polycaprolactone–collagen (PCL–C)

to create a potential wound care material. Researchers used a PCL–C (1 : 1 (w/w)) solution to develop electrospun matrices. The insulin-loaded nanoparticles were created using the ionic gelation procedure and then adhered to the strands. Numerous dressing characteristics were examined, including surface wettability, water vapor permeability, blood compatibility, and mechanical qualities. They employed a full-thickness excisional wound model to evaluate the *in vivo* healing potential of the dressings. Their findings showed that the manufactured scaffolds could help treat wounds in clinical settings. According to their research, adding insulin–chitosan particles improved blood compatibility, water absorption, and PCL–C hydrophilicity. Based on the macroscopic and histological findings, the insulin-containing dressing performed better than the PCL–C and negative control groups in wound healing. The advanced nanofiber material had a beneficial impact on the healing of wounds.[194]

5.2. Hemostatic dressings

Recently, several hemostatic dressings based on chitosan have been created. Because of their ability to produce cationic clusters that can interact with anions on red blood cells, CS nanofibers have exceptional hemostatic capabilities that may finally limit blood loss.[216] This is accomplished by speeding up platelet and red blood cell aggregation.[217] This technique is also successful even in individuals with coagulation abnormalities. It is independent of the patient's clotting system. By electrospinning, Ren and colleagues created a medicinal dressing made of silk fibroin, chitosan, and halloysite nanotubes.[218] Electrospun CS composite membranes also demonstrated better blood coagulation rates, improved tensile properties, and antibacterial activity, all of which suggest their potential value as a medical dressing. An anti-fibrinolytic medication known as tranexamic acid (TXA) is often used in trauma surgery and has been found to improve wound healing.[219]

Sasmal and colleagues created TXA-loaded CS–PVA electrospun nanofibers for hemorrhage control applications. The findings support the function of chitosan in hemostasis by showing that the entire blood-clotting duration of pure CS–PVA nanofibrous membranes reduced from 210 ± 10 s to 167 ± 6 s with an increasing amount of CS. Additionally, clotting time and plasma recalcification time were dramatically shortened when TXA was added to CS nanofibers, demonstrating the enormous potential of TXA-loaded CS nanofibers for managing civil and military hemostasis. Additionally, Leonhardt and colleagues observed the development of nanostructures in chitosan mats by assembling CS inside a hydrogel carrier template produced from cyclodextrin by proton exchange and complexation. The assembled CS was highly entangled with 9.2 ± 3.7 nm nanofiber diameters and a macroscopic shape resembling a honeycomb. Compared to commercially available absorbable hemostatic dressings, the CS-based composite hydrogels result in significantly less blood loss and faster time to hemostasis.

5.3. Thrombolytic potential

A blood clot, also known as a thrombus, can develop within the body's vascular system and obstruct the flow of blood vessels.

Thrombosis is a prevalent underlying pathology that can lead to severe cardiovascular disorders, including myocardial infarction, ischemic stroke, and venous thromboembolism, which can be life-threatening. Thrombotic occlusions of blood vessels can significantly contribute to high morbidity and mortality rates. The main thrombolytic drugs, such as urokinase and streptokinase, have certain limitations that restrict their clinical usage. These limitations include a lack of targeting, severe side effects, and a short half-life.[220] Nano-drug delivery systems are expected to resolve such problems, and researchers have investigated several methods, such as biological and physical-responsive systems. Nanofibers were created using electrospinning to encapsulate biomolecules, demonstrating their antithrombotic properties. Chitosan is a hydrophilic polysaccharide with cationic properties that is obtained from chitin. It can create polyelectrolyte complexes when combined with molecules with a negative charge.[221] Chitosan nanoparticles were created through self-assembly by using ionic crosslinking with sodium tripolyphosphate. These nanoparticles had a size of 236 nm and were loaded with urokinase, achieving an encapsulation efficiency of 95%.[222] The efficacy of intravenous injections and catheter-driven drug delivery was evaluated in thrombin-induced rabbit venous thrombosis. The results showed that catheter-driven drug delivery had superior thrombolytic efficacy to free urokinase. Liao *et al.* covalently grafted cRGD onto – *N,N,N*-trimethyl chitosan (TMC), the quaternized chitosan derivative. This targeted GPIIb and IIIa receptors, as TMC has superior solubility and elevated charge density. The cRGD-LK-NPs were created by combining lumbrokinase (LK) with sodium tripolyphosphate through ionic gelation. These nanoparticles significantly enhanced thrombolysis in clot-occluded tubes and a $FeCl_3$ rat carotid artery model when administered at 90 000 U kg^{-1} of LK. We evaluated the antithrombotic properties of the nanofibrous scaffolds by measuring the activated partial thromboplastin times (APTT) before and after heparinization to determine the clotting time.[223] The APTT values of the uniform CS/PCL were 29.7 ± 4.5 s, and the APTT values of the gradient CS/PCL were 36.7 ± 3.2 s before heparinization. During the standard test period, the APTT values of heparinized gradient CS/PCL and uniform CS/PCL were longer than 180 seconds. The results indicate that heparinization significantly improved the anticoagulation of the nanofibrous scaffolds.[224] Chitosan can undergo chemical modifications resulting in soluble derivatives, expanding its potential applications. Chitosan's acylated derivatives exhibit solubility in chloroform, benzene, and tetrahydrofuran (THF). As the concentration of H-chitosan increases, the average diameter of ultrathin fibers obtained from chloroform increased. H-Chitosan is a highly intriguing derivative of chitosan that holds great potential for utilization in various biomedical applications due to its resistance to hydrolysis by the lysosome and its anti-thrombogenic properties.[225]

5.4. Bone regeneration

The vast, rigid connective tissue called bone provides the body's structural integrity and support for many internal organs.[226] One of the biggest problems brought on by infections and trauma is regarded as defects in giant bones; still, researchers

must resolve restrictions and downsides in bone tissue engineering despite many attempts, including those using bone grafts and implants. Bone tissue engineering has been touted as a potential replacement for conventional treatments throughout the last several decades. A good scaffold design that can control bone healing and replicate the function of the ECM in bone tissue is one of the essential components of bone tissue engineering (Table 4). So, scaffolds should be made from biodegradable and biocompatible materials with the proper porosity, pore size, mechanical properties, and osteoconductivity.[227] In situ, coprecipitation synthesis and electrospinning were used by Zhang et al. to construct a biomimetic nanocomposite nanofiber of hydroxyapatite and chitosan (HAp–CS). Coprecipitation created a HAp–CS nanocomposite with spindle-shaped HAp nanoparticles evenly dispersed throughout the chitosan matrix. Researchers have developed continuous HAp–CS nanofibers, and the HAp nanoparticles were integrated into the electrospun nanofibers by utilizing a tiny quantity of ultra-high molecular weight PEO as a fiber-formation aiding additive. Human fetal osteoblast cells were cultured in vitro for up to 15 days. It was shown that adding HAp nanoparticles to chitosan electrospun nanofibers significantly increased bone formation compared to pure electrospun scaffolds.[228] Throughout a reductive alkylation procedure, Nourmohammadi et al. mixed chitosan with varying quantities of oxidized starch. Then, chopped calcium phosphate-coated polycaprolactone nanomaterials are introduced to the chitosan-starch composite scaffolds to acquire bioactivity and replicate the bone ECM structure.

According to SEM findings, each platform exhibited a solidly linked, porous structure. The median pore size, porosity, and water permeability of the composite scaffolds rose with greater starch incorporation, whereas the trend for stiffness and compressive modulus was the reverse. It was discovered via the cultivation of osteoblast-like cells (MG63) upon these scaffolds that a more excellent starch content increased cell viability. In addition, the cells covered the platforms in a single layer by spreading and adhering well. The standard cholesterol-lowering drug simvastatin has demonstrated a promising capacity for bone repair. Ghadri et al.[229,230] examined simvastatin-loaded chitosan (CS) nanofibrous membranes for the guided regeneration of bones and their ability to promote bone growth in rat calvarial defects. Using an electrospinning process, they created nanofibrous CS membranes with a random fiber orientation and then put simvastatin into them in a sterile environment. An implanted membrane covered a critical-sized calvarial deficiency with an 8 mm diameter. Simvastatin-loaded CS membranes were utilized as the experimental material, and two groups were employed as controls (non-loaded CS membranes).

Using micro-computed tomography (micro-CT), researchers looked at the growth of bone from a histological point of view at 4 and 8 weeks. Both groups had excellent biocompatibility throughout the healing period, with only a mild to moderate inflammatory response. The histology and micro-CT analysis findings demonstrated that the reference and experimental membranes formed bone in calvarial lesions as early as 4 weeks.

At 8 weeks, the histology findings in both groups revealed newly created bone bridges, consolidating calvarial deficiencies, and partial radiographic defect coverage. As a protective barrier for guided bone healing applications, biodegradable CS nanofibrous membranes containing simvastatin displayed a high regenerative ability. Due to these membranes' large surface area, nanofibers could be used to distribute biological mediators to specific regions. The surgical method known as guided bone regeneration (GBR) is routinely used to improve the alveolar bone abnormalities typically seen in patients who are missing teeth.

Various non-resorbable and resorbable barrier membranes are employed in GBR treatments to stop soft tissue infiltration and promote the creation of skeletal tissue.[230] The stability and characteristics of surface butyrylated chitosan (BCS) nanofiber membranes have recently been enhanced by Wu et al., exploding their potential in GBR. Compared to unmodified fibers in aqueous conditions, the produced (BCS) membranes demonstrated an overall degree of substitution of 1.61, an average diameter of 99.3 nm, a 75% reduction in swelling, and a doubling in suture pull-out strengths. Researchers discovered the BCS nanofiber membranes to be cell occlusive and enhance

Table 4 Chitosan electrospun nanofibers for bone regeneration applications

Nanofiber materials	Electro spinning	Solvents	Electrospinning setting			Diameter (nm)	Biocompatibility (target cell line)	Ref.
			kV	cm	mL h^{-1}			
Simvastatin-loaded CS nanofibers	Single nozzle	TFA: methylene chloride	25	15	20 μL min^{-1}	24.79 ± 10.72	Rodent calvarial defects	Ghadri et al. (2018)[230]
Poly(glycerol sebacate)/PCL/CS	Single nozzle	Chloroform Methanol	18	16	1	605 ± 121	Human fetal osteoblasts (hFOB)	Rad et al. (2017)[233]
PCL/carboxymethyl CS	Single nozzle	Acetic acid Formic acid	18–30	16–20	0.1–0.7	356	Human osteoblast cells (MG63)	Sharifi et al. (2018)[234]
PCL nanofibers-CS-oxidized starch	Single nozzle	Acetic acid Formic acid	11	10	0.4	545	Human osteoblast-like cells, MG63	Nourmohammadi et al. (2016)[227]
CS/PLA nanofibers	Emulsion	Chloroform	17	15	0.012 mL min^{-1}	200	TLR4 of human periodontal ligament cells	Shen et al. (2018)[176]
Hydroxyapatite-hybridized CS/chitin whisker bio nanofibers	Single nozzle	Deionized water	18	15	0.05	550	Osteoblast cells	Pangon et al. (2016)[235]
Butyrylated CS nanofiber	Single nozzle	TFA	25	15	1.2	99.3 ± 33.7	NIH 3T3	Wu et al. (2017)[231]

fibroblasts' adhesion and growth *in vitro*. The BCS nanofiber membranes were found to have a significantly better protective barrier than commercially available collagen membranes *in vivo*, with little soft tissue permeation through the membranes, and to dramatically accelerate bone regeneration in a rat calvarial critical-size abnormality over a 12 week healing period. They discovered that BCS nanofibers had enhanced stability in an aquatic medium with less swelling, better fiber shape, and stable mechanical characteristics than unmodified CS nanofibers.[231] Jin *et al.* created a bioactive calcium phosphate–chitosan (CaP CS/Ag) membrane loaded with silver ions. Nanofibers mimicked the extracellular matrix structure of the produced fibrous membranes. The addition of CaP considerably improved the membranes' capacity for mineralization. *Staphylococcus mutans* could not adhere to and develop on CaP–CS/Ag membranes due to a sustained release of silver ions. Cell adhesion and MTT test findings demonstrated that bone marrow stromal cells were compatible with CaP–CS/Ag membranes. CaP–CS/Ag nanofibrous membranes created using electrospinning have a lot of promise for application in directed bone tissue regeneration.[232]

5.5. Vascular tissue engineering

The most significant cause of mortality and disability globally is cardiovascular disease. Implanting conduits is the standard method of treating cardiovascular problems.[236,237] Graft materials often employed include artificial grafts, allografts, autologous tissues, and xenografts. These materials might, however, result in issues, including thrombogenicity and infection. A different approach to treating cardiovascular disorders is provided by vascular tissue engineering. Numerous research teams have looked at employing vascular growth factors to treat cardiovascular disease.[238–242] By combining biodegradable scaffolds with autologous cells, vascular tissue engineering aims to create vascular building materials identical to the natural vessel.[243,244] The scaffolding materials should assist the attachment and growth of the cells and be biodegradable, biocompatible, and non-immunogenic.[245–247] In recent years, vascular tissue engineering has extensively used nanostructured scaffold materials made by electrospinning.[248,249] For use in vascular tissue engineering, synthetic polymers and biopolymers such as PGA, PLA, PCL, collagen, silk, and chitosan in the form of nanoparticles

have been studied (Table 5).[250–253] Electrospun chitosan-based nanofibers were used as scaffolds in vascular tissue engineering.[254] To avoid thrombosis, the researchers created a 3D gradient heparinized chitosan and poly-3-caprolactone (CS–PCL) nanofibrous platform with VEGF. After 72 hours of growth, human umbilical vein endothelial cells (HUVECs) produced a significant amount of F-actin, indicating that actin lanes had developed in the networks and around the perimeter of each cell. Additionally, compared to homogeneous scaffolds, the lumen surface of gradient scaffolds showed higher levels of von Willebrand factor (vWF) expression from HUVECs. Gradient CS–PCL, therefore, promoted HUVEC proliferation and triggered quick endothelialization. Additionally, compared to the uniform CS–PCL scaffold, the release behavior of VEGF from the gradient CS–PCL scaffold was much steadier and more continuous.

5.6. Neural tissue engineering

The peripheral and central nervous systems are both parts of the nervous system.[255] The patients experience pain from injuries or neurological systems.[256] Due to the nervous system's low capacity for regeneration, therapy is complicated. Autologous, allogeneic, xenogeneic, and other treatments may result in issues such as immunological rejection and disease transmission.[257,258] New methods for brain regeneration are made possible by developments in neural tissue engineering.[259] A biodegradable and biocompatible scaffold with excellent porosity and proper mechanical strength is needed in neural tissue engineering to enable brain regeneration. Researchers used self-assembled and electrospun nanofibrous materials in neural regeneration because they might help neurites and axons grow back.[260–262] Chitosan nanoparticles have been created recently to provide new opportunities for creating scaffolds in regenerative brain medicine and tissue engineering (Table 5).[263,264] Chitosan and poly-3-caprolactone (CS–PCL) platforms were made, and their potential for application in nerve regeneration was examined by Cooper *et al.*[265] Pictures were taken using a scanning electron microscope show aligned nanobeads with an average diameter of 408 nm and randomly oriented nanobeads with an average diameter of 405 nm. To investigate the possible use of CS–PCL nanoparticles in nerve regeneration, researchers chose neuron-like PC-12 cells. After being grown for 7 days, the PC-12 cells adhered effectively to randomly distributed and aligned CS–PCL nanoparticles. In

Table 5 Challenges and possible solutions

S. no.	Challenges	Possible solutions
1	Complex tissue engineering	3D printing can construct complex organ structures
2	Impact the dimensions and shape	3D printing techniques can overcome these difficulties
3	Chitosan antimicrobials nanofibrous dressings	Preclinical and clinical investigations needed
4	Completely degraded during wound healing	It needs ultra-fine tuning of molecular weight and fiber diameter
5	Strong antibacterial, antioxidant, and anti-inflammatory characteristics required	More detailed research and fundamental steps need to be undertaken
6	Improve cell infiltration	Multiple-layer membranes are an effective solution
7	Reconstructing multi-layered structures is difficult	Skin replacement should mimic tissue layers' thickness and structure
8	ROS delay in wound healing	Membrane-loaded cerium oxide NPs and enzyme mimetic particles are useful
9	A rigid membrane to the wound would be difficult	On wounds, bioactive chitosan electrospinning is effective
10	Lose functionality due to temperature, moisture, or pH	It needs fiber shape and chemical configuration control

contrast to arbitrarily oriented nanofibers, the cells on the aligned CS–PCL nanofibers exhibited parallel proliferation along the nanofiber direction and longer neurites similar to the nanofibers. Additionally, PC-12 cells were used to assess the expression of genes for β-tubulin and neurofilament−200 (NF-200) on nanoparticles. On aligned and randomly distributed nanofibers, PC-12 cells produced about the exact amounts of NF200, indicating that the cells differentiated well there. PC-12 cells expressed almost three times as much β-tubulin on aligned nanofibers as on randomly oriented nanofibers, which showed that their neurites were longer.

Additionally, chitosan nanofibers were created utilizing deacetylation and self-assembly methods.[266] Poly-D-lysine (PDL) was combined with chitosan nanoparticles with 4 nm and 12 nm diameters to test the capacity to promote cell attachment, neurite coverage, and survival. According to the findings, neurons grown on 4 nm chitosan nanofiber scaffolds demonstrated substantial neurite extension and arborization since day 3 compared to day 1. Still, no additional neurite elaboration was seen on the 12 nm nanofiber surface. After 7 days of culture, 37.9% of the neurons on the 4 nm chitosan nanoparticles with PDL were still alive, while only 13.5% were alive on the conventional PDL surfaces, showing that neurons significantly improve the long-term viability of the cells.

5.7. Cosmeceuticals

Recent developments in nanomaterials and biotechnology have made chitosan and its derivatives one of the natural materials of interest for application in cosmeceuticals. Due to their potential anti-aging properties, these substances may serve as nanocarriers for active ingredients in personal care and cosmetic products or as agents for maintaining oral hygiene.[267,268] Chitosan's inherent antioxidant activity is advantageous for skincare products.[269] The antioxidative carboxylation of chitosan stops the activity of matrix metalloproteinases (MMPs), which break down the collagen matrix of connective tissues and protect against reactive oxygen species (ROS), damaging tissues during radiation therapy, sunburn, and other types of biological stress.[270] Chitosan nanoparticles and microparticles are now often used in oral care products like toothpaste and mouthwash because they kill bacteria very well, especially *S. mutans*, which is a significant cause of tooth decay.[271,272] Chitosan and its derivatives may also interact with keratin to generate elastic and durable films that shield against wear and injury on individual hair strands, improving the look and conditioning of hair.[273] While chitosan derivatives have been used as cutting-edge materials in producing various cosmeceutical goods; chitosan nanofibers are only used in a small number of these items. To the authors' knowledge, a chitin nanofibril mask intended to be used as a facial dressing for medicinal reasons is the only cosmetic item reported to use these nanofibers.

The nano/micropores in this product enable bioactive substances to pass through the dressing while preventing microbes and contaminants from getting to the skin's healing tissues.[274] This mask is said to be fashioned from a thin, flexible, transparent film that is cast. Chitosan derivatives and nanofibrous chitosan may be utilized to create dressing scaffolds with specific antioxidant and antibacterial characteristics. By electrospinning or blow spinning, researchers can create skin-friendly dressing filters based on those nanofiber membranes, producing a functionalized nanofiber layer for tissue regeneration, skin therapy, and other cosmeceutical applications. These filters generally contain preservatives, drugs, and active healing agents.

5.8. Biosensors

Electrospun nanofiber materials have recently received a great deal of attention for their potential use in biosensors due to the high specific surface area, polymer diversity, flexible 3D porous structures of nanofiber materials, including fiber diameter, product thickness, porosity, and pore size, controllable performance, and process simplicity. Nanofiber-based biosensors are superior to conventional biosensors because they are very responsive, susceptible, capable of detecting a wide range of objects, and more affordable. Additionally, biopolymer-based or doped electrospun materials are biocompatible. For the immobilisation of enzymes, a nanofibrous CS-PVA membrane was constructed.[275] The benefits of this chitosan nanofibrous membrane for lipase immobilization include high enzyme loading of up to 63.6 mg g^{-1} and activity retention of 49.8%.

Researchers improved immobilized lipase's stability toward pH, temperature, reuse, and storage. These findings suggest that the exceptional biocompatibility of the CS nanofibrous membranes makes them a good support for enzyme immobilization. Applications for biosensors may leverage this technology.

5.9. Filtration

Compared to nanofibers from other synthetic polymers, chitosan-based ones exhibit the necessary filtering characteristics. They were employed in various filtration applications, including media for air filters and water purification systems.[276] Desai *et al.* created a nanofibrous filter medium by electrospinning chitosan/PEO mix solutions onto a spun-bonded nonwoven polypropylene substrate. They showed how to use chitosan-based nanofiber filter media to efficiently remove contaminated particle media, pathogenic microorganisms, and heavy metal ions from water and air media. Researchers have examined the effectiveness of these chitosan-based filter media's heavy metal binding, antimicrobial properties, and physical filtering. These results were associated with these nanofiber filter media's surface chemical and physical traits. The surface chitosan concentration and fiber size significantly impacted the nanofiber mats' ability to filter. Nanofibrous filter media made of chitosan showed hexavalent chromium binding capabilities of up to 35 mg chromium/g chitosan and a 2–3 log decrease in *E. coli* bacteria. The chitosan blend fibers did exhibit a 2–3 log decrease in *E. coli* after 6 hours of contact time. When tested using aerosol and PS beads floating in the water, the nanofibrous filter media's water and air filtration efficiency revealed high efficiencies associated with the fibrous media's size and shape. These findings demonstrated chitosan nanofiber filters' usefulness and utility in commercial settings. Chitosan electrospun nanofiber mats with a diameter of around ∼235 nm were tested in an aqueous solution for their capacity to bind metals.[277]

The chitosan nanofiber mats demonstrated excellent erosion stability in water and a strong adsorption affinity for metal ions in aqueous solutions after being neutralized with potassium carbonate. The adsorption outcomes of Cu(II) and Pb(II) closely resemble the Langmuir isotherm, suggesting that the nanofiber mats' adsorption process was limited to a monolayer. The equilibrium adsorption capacities of Cu(II) and Pb(II) were found to be 485.44 mg g^{-1} and 263.15 mg g^{-1}, respectively. The published maximum values of chitosan microspheres (80.71 mg g^{-1})[278] and plain chitosan (45.20 mg g^{-1})) were, respectively, $\sim$6 and $\sim$11 times lower than the Cu(II) adsorption results. The electrospun nanofiber mats made of chitosan exhibit a notable capacity for adsorption, indicating their potential for effectively filtering and neutralizing hazardous metal ions and microorganisms. Furthermore, these mats retain chitosan's inherent properties, including biocompatibility, non-antigenicity, bioactivity, hydrophilicity, and non-toxicity.

6. Conclusions

More research is needed to move these materials from the laboratory to clinical applications. Although researchers have been able to modify the instrumentation and solution variables to replicate the structure and morphology of natural tissues, these processes still require additional characterization, including being put through clinical trials, before researchers can use them confidently in applications for the treatment of medical diseases. Manufacturers may have even more control over the final template by using electrospinning and enhancing it with additives. Additionally, physicians and bioengineers may tackle unsolved regenerative treatments by tailoring the fibers' diameters, sizes, morphologies, and orientations to the therapeutic application. The destiny of electrospinning of these composites will be significantly influenced by replicating actual tissues' functional and structural characteristics. The preparation procedures, fiber configurations, material choices, target applications, and spinning method choices are all aspects of electrospinning that should be considered. The materials and fiber geometries have significantly expanded in variety due to the fast advancement of electrospinning, and their biological applications are also increasing. Researchers developed this technology to create fibrous constructions with topographical clues to cell alignment orientation.

Electrospinning in conjunction with 3D printing technology will enable the creation of complex organ structures, even though neuronal and vascular architecture and many heterogeneous cells present significant problems in intricate bioengineering and organ models. Future research should focus on developing 3D scaffolds combined with growth factors, high viability cells, and enhanced infiltration. Therefore, a new era of tissue and organ rejuvenation will be ushered in by ongoing research and development as well as the creation of cutting-edge electrospinning technologies. The current review reveals a lot of scientific data available to support the essential characteristics and biocompatibility of chitosan electrospun

composite biomaterials for various purposes in tissue engineering and regenerative medicine. Several biocompatible and biodegradable synthetic materials might be directly electrospun into nanofibers for application in tissue engineering via electrospinning.

7. Future perspective

The creation of multicomponent, multifunctional nanofiber systems based on chitosan has recently made great strides. It is currently a regular practice to functionalize these fibers with different bioactive medications, targeted therapies, and conductive or magnetic components to further enhance and fine-tune the capabilities of chitosan and its derivatives. Even though these technologies are already accessible, difficulties still exist since incorporating materials might cause applications to lose functionality if the processing environment's temperature, moisture, or pH is sensitive to them. Therefore, chitosan-based fibers still need to be developed and tested for enhanced functionality as commercial items used in everyday life and medical devices. It is yet to be discovered how these fiber materials' physical qualities and biological traits relate to one another on all scales. Advanced nanofiber configurations, such as core–sheath nanofibers, aligned nanofibers, and gradient nanofibers, exhibit various mechanical and biological characteristics, for instance. Controlling the physical shapes and chemical configurations of these fibers is required to design advanced materials with excellent nanoscale properties, such as controlled-release capabilities, the guiding of cell migration and adhesion conductivity and magnetism for biomedical purposes, improved strength and elasticity, and possibly nanoscale self-assembly and self-disassembly for injectable biomedical remedies and perpetual sustainment. Additional post-spinning processes may help enhance fiber adhesion, resulting in better textiles for applications such as intelligent apparel, food packaging, and biomedical applications. Each surface modification technique has the potential to lead to the creation of fibrous scaffolds with many functions. Further consideration is necessary because chitosan-based products are biodegradable.

The degradation of chitosan-based fibrous materials may be adjusted since the degradation profile is directly connected to the polymer's specific chemical composition and the fibers' hierarchical architecture. This feature offers considerable potential for sustainable food, cosmeceutical, and medicinal uses, mainly if it can be regulated and activated. Tissue engineering is a significant area where chitosan-based nanofibers will be used. For the treatment of wounds and as replacements for tissue grafts, materials scientists are developing ever-more sophisticated materials. Although fiber spinning is undoubtedly a flexible method for producing sub-micron fibers, it still has drawbacks, such as the issues with repeatability brought on by the massive number of regulated factors that ultimately affect the dimensions and shape of the desired result. We will likely see a shift from the use of collagen fibers for medical use in favor
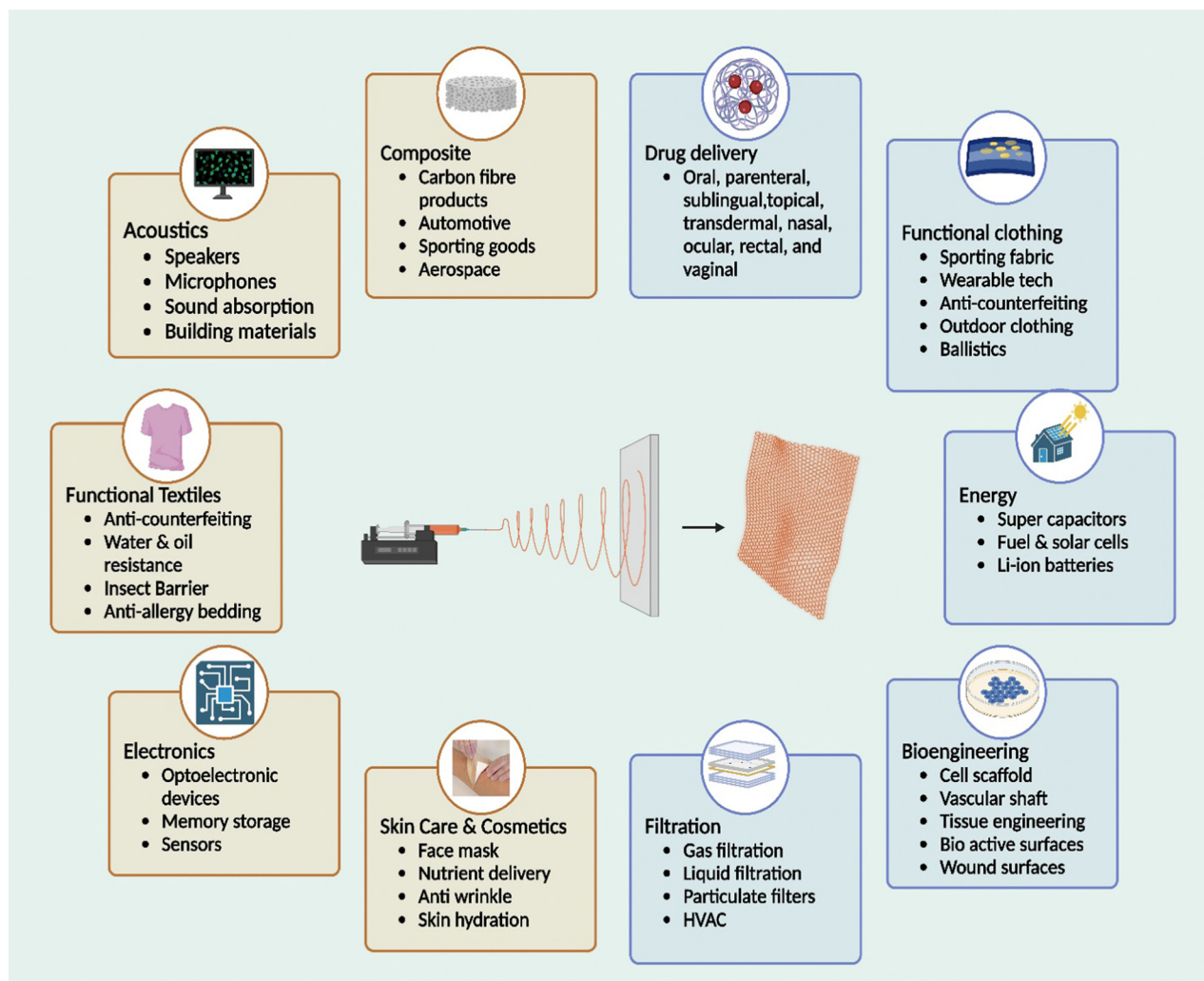
Fig. 8 Application of electrospun nanofibres in different fields (modified from source ref. 279).

of more sustainable biomaterials like chitosan because of increased regulatory restrictions, particularly in Europe, the European Tissue and Cells Directive, and the new Medical Device Regulation MDR. Multidimensional chitosan-based materials with structures that resemble specific characteristics of actual tissues might be created with a combination of cutting-edge fabrication techniques such as sub-micron fiber spinning and 3D printing techniques. These materials have shown exceptional biological features in addition to having great compressive strength, viscoelastic capabilities, and the ability for sustained release and resorption.

These characteristics make chitosan-based materials appropriate as a starting point for creating the newest class of intelligent materials for use in tissue engineering. Although chitosan-based micro- and nanofibers have successfully scaled up and entered several clinical studies, problems with the large-scale manufacturing of sub-micron chitosan fibers remain. Commercially successful in the medical sector, sub-micron chitosan fibers must overcome difficulties such as homogeneity of raw resources, repeatability,

regulatory barriers, and manufacturing expense. Table 5 demonstrates challenges and possible solutions for future work. Fig. 8 illustrates the application of electrospun nanofibers in various fields.

Author contributions

Conceptualization, G. P. T., G. S., V. R. S.; validation, G. P. T., G. S., and V. R. S.; writing—original draft preparation, G. P. T., G. S.; writing, review and editing, S. G., V. R. S.; visualization, K. M., V. A., and S. G.; supervision, K. M., V. A., and V. R. S. All authors have read and agreed to the published version of the manuscript.

Conflicts of interest

There are no conflicts to declare.

Acknowledgements

References

1 K. Kalantari, A. M. Afifi, H. Jahangirian and T. J. Webster, *Carbohydr. Polym.*, 2019, **207**, 588–600.

2 A. Madni, R. Kousar, N. Naeem and F. Wahid, *J. Bioresour. Bioprod.*, 2021, **6**, 11–25.

3 N. Morin-Crini, E. Lichtfouse, G. Torri and G. Crini, *Environ. Chem. Lett.*, 2019, **17**, 1667–1692.

4 P. Sahariah and M. Másson, *Biomacromolecules*, 2017, **18**, 3846–3868.

5 Ö. V. Rúnarsson, J. Holappa, T. Nevalainen, M. Hjálmarsdóttir, T. Järvinen, T. Loftsson, J. M. Einarsson, S. Jónsdóttir, M. Valdimarsdóttir and M. Másson, *Eur. Polym. J.*, 2007, **43**, 2660–2671.

6 C. K. S. Pillai, W. Paul and C. P. Sharma, *Prog. Polym. Sci.*, 2009, **34**, 641–678.

7 P. Sahariah, V. S. Gaware, R. Lieder, S. Jónsdóttir, M. Hjálmarsdóttir, O. E. Sigurjonsson and M. Másson, *Mar. Drugs*, 2014, **12**, 4635–4658.

8 J. Holappa, M. Hjálmarsdóttir, M. Másson, Ö. Rúnarsson, T. Asplund, P. Soininen, T. Nevalainen and T. Järvinen, *Carbohydr. Polym.*, 2006, **65**, 114–118.

9 L. Wei, W. Deng, S. Li, Z. Wu, J. Cai and J. Luo, *J. Bioresour. Bioprod.*, 2022, **7**, 63–72.

10 E. M. Saad, R. F. Elshaarawy, S. A. Mahmoud and K. M. El-Moselhy, *J. Bioresour. Bioprod.*, 2021, **6**, 223–242.

11 J. K. Park, M. J. Chung, H. N. Choi and Y. Il Park, *Int. J. Mol. Sci.*, 2011, **12**, 266–277.

12 P. S. Bakshi, D. Selvakumar, K. Kadirvelu and N. S. Kumar, *Int. J. Biol. Macromol.*, 2020, **150**, 1072–1083.

13 Z. Zakaria, Z. Izzah, M. Jawaid and A. Hassan, *BioResources*, 2012, **7**, 5568–5580.

14 M. Kaliva, A. Georgopoulou, D. A. Dragatogiannis, C. A. Charitidis, M. Chatzinikolaidou and M. Vamvakaki, *Polymers*, 2020, **12**, 316.

15 Z. Yaneva, D. Ivanova, N. Nikolova and M. Tzanova, *Biotechnol. Biotechnol. Equip.*, 2020, **34**, 221–237.

16 J. Nilsen-Nygaard, S. P. Strand, K. M. Vårum, K. I. Draget and C. T. Nordgård, *Polymers*, 2015, **7**, 552–579.

17 A. Martinez, E. Chornet and D. Rodrigue, *J. Texture Stud.*, 2004, **35**, 53–74.

18 L. Ren, J. Xu, Y. Zhang, J. Zhou, D. Chen and Z. Chang, *Int. J. Biol. Macromol.*, 2019, **135**, 898–906.

19 F. A. Razmi, N. Ngadi, S. Wong, I. M. Inuwa and L. A. Opotu, *J. Cleaner Prod.*, 2019, **231**, 98–109.

20 J. M. F. Pavoni, C. L. Luchese and I. C. Tessaro, *Int. J. Biol. Macromol.*, 2019, **138**, 693–703.

21 B. Kaczmarek, A. Owczarek, K. Nadolna and A. Sionkowska, *Mater. Lett.*, 2019, **245**, 22–24.

22 E. Zhang, R. Xing, S. Liu, Y. Qin, K. Li and P. Li, *Carbohydr. Polym.*, 2019, **222**, 115004.

23 A. K. Sah, M. Dewangan and P. K. Suresh, *Colloids Surf., B*, 2019, **178**, 185–198.

24 A. Barra, Z. Alves, N. M. Ferreira, M. A. Martins, H. Oliveira, L. P. Ferreira, M. M. Cruz, M. D. D. Carvalho, S. M. Neumayer, B. J. Rodriguez, C. Nunes and P. Ferreira, *J. Mater. Chem. B*, 2020, **8**, 1256–1265.

25 R. A. A. Muzzarelli, *Cell. Mol. Life Sci.*, 1997, **53**, 131–140.

26 Y. Pang, A. Qin, X. Lin, L. Yang, Q. Wang, Z. Wang, Z. Shan, S. Li, J. Wang, S. Fan and Q. Hu, *Oncotarget*, 2017, **8**, 35583–35591.

27 C. M. Lehr, J. A. Bouwstra, E. H. Schacht and H. E. Junginger, *Int. J. Pharm.*, 1992, **78**, 43–48.

28 A. Jintapattanakit, V. B. Junyaprasert and T. Kissel, *J. Pharm. Sci.*, 2009, **98**, 4818–4830.

29 C. Federer, M. Kurpiers and A. Bernkop-Schnürch, *Biomacromolecules*, 2021, **22**, 24–56.

30 A. Sood, A. Dev, S. J. Mohanbhai, N. Shrimali, M. Kapasiya, A. C. Kushwaha, S. Roy Choudhury, P. Guchhait and S. Karmakar, *ACS Appl. Nano Mater.*, 2019, **2**, 6409–6417.

31 J. P. Venter, A. F. Kotzé, R. Auzély-Velty and M. Rinaudo, *Int. J. Pharm.*, 2006, **313**, 36–42.

32 E. Khor, *Curr. Opin. Solid State Mater. Sci.*, 2002, **6**, 313–317.

33 Y. Maeda, R. Jayakumar, H. Nagahama, T. Furuike and H. Tamura, *Int. J. Biol. Macromol.*, 2008, **42**, 463–467.

34 M. C. Gortari and R. A. Hours, *Electron. J. Biotechnol.*, 2013, **16**, 717–3458.

35 T. Dai, M. Tanaka, Y. Y. Huang and M. R. Hamblin, *Expert Rev. Anti-Infect. Ther.*, 2011, **9**, 857–879.

36 R. Jayakumar, M. Prabaharan, P. T. Sudheesh Kumar, S. V. Nair and H. Tamura, *Biotechnol. Adv.*, 2011, **29**, 322–337.

37 F. L. Mi, S. S. Shyu, C. T. Chen and J. Y. Schoung, *Biomaterials*, 1999, **20**, 1603–1612.

38 A. Miwa, A. Ishibe, M. Nakano, T. Yamahira, S. Itai, S. Jinno and H. Kawahara, *Pharm. Res.*, 1998, **15**, 1844–1850.

39 E. Khor and L. Y. Lim, *Biomaterials*, 2003, **24**, 2339–2349.

40 J. Venkatesan and S. K. Kim, *Mar. Drugs*, 2010, **8**, 2252–2266.

41 J. Y. Hao, F. L. Mi, S. S. Shyu, Y. B. Wu, J. Y. Schoung, Y. H. Tsai and Y. Bin Huang, *J. Biomed. Mater. Res.*, 2002, **59**, 438–449.

42 T. Huq, A. Khan, D. Brown, N. Dhayagude, Z. He and Y. Ni, *J. Bioresour. Bioprod.*, 2022, **7**, 85–98.

43 M. Sukul, P. Sahariah, H. L. Lauzon, J. Borges, M. Másson, J. F. Mano, H. J. Haugen and J. E. Reseland, *Carbohydr. Polym.*, 2021, **254**, 117434.

44 W. Cao, D. Jing, J. Li, Y. Gong, N. Zhao and X. Zhang, *J. Biomater. Appl.*, 2005, **20**, 157–177.

45 N. D. Tien, S. P. Lyngstadaas, J. F. Mano, J. J. Blaker and H. J. Haugen, *Molecules*, 2021, **26**, 2683.

46 G. Sabarees, G. P. Tamilarasi, V. Velmurugan, V. Alagarsamy, B. Z. Sibuh, M. Sikarwar, P. Taneja, A. Kumar and P. K. Gupta, *J. Drug Delivery Sci. Technol.*, 2022, **79**, 103994.

47 G. P. Tamilarasi, M. Krishnan, G. Sabarees and S. Gouthaman, *Appl. Nanobiomater.*, 2022, **3**, 202–232.

48 S. K. Shukla, A. K. Mishra, O. A. Arotiba and B. B. Mamba, *Int. J. Biol. Macromol.*, 2013, **59**, 46–58.

49 R. Jayakumar, D. Menon, K. Manzoor, S. V. Nair and H. Tamura, *Carbohydr. Polym.*, 2010, **82**, 227–232.

50 G. Kravanja, M. Primožič, Ž. Knez and M. Leitgeb, *Molecules*, 2019, **24**, 1960.

51 M. N. V. Ravi Kumar, *React. Funct. Polym.*, 2000, **46**, 1–27.

52 T. U. Rashid, M. M. Rahman, S. Kabir, S. M. Shamsuddin and M. A. Khan, *Polym. Int.*, 2012, **61**, 1302–1308.

53 H. Amiri, M. Aghbashlo, M. Sharma, J. Gaffey, L. Manning, S. M. Moosavi Basri, J. F. Kennedy, V. K. Gupta and M. Tabatabaei, *Nat. Food*, 2022, **3**, 822–828.

54 I. Younes and M. Rinaudo, *Mar. Drugs*, 2015, **13**, 1133–1174.

55 A. Tolaimate, J. Desbrieres, M. Rhazi and A. Alagui, *Polymer*, 2003, **44**, 7939–7952.

56 A. Greiner and J. H. Wendorff, *Angew. Chem., Int. Ed.*, 2007, **46**, 5670–5703.

57 H. Kadavil, M. Zagho, A. Elzatahry and T. Altahtamouni, *Nanomaterials*, 2019, **9**, 77.

58 G. P. Tamilarasi, G. Sabarees, K. Manikandan, S. Gouthaman, V. Alagarsamy and V. R. Solomon, *Mini-Rev. Med. Chem.*, 2023, DOI: 10.2174/1389557523666230221155544.

59 C. K. S. Pillai, W. Paul and C. P. Sharma, *Prog. Polym. Sci.*, 2009, **34**, 641–678.

60 S. De Vrieze, P. Westbroek, T. Van Camp and L. Van Langenhove, *J. Mater. Sci.*, 2007, **42**, 8029–8034.

61 J. D. Schiffman and C. L. Schauer, *Biomacromolecules*, 2007, **8**, 594–601.

62 L. L. Min, Z. H. Yuan, L. Bin Zhong, Q. Liu, R. X. Wu and Y. M. Zheng, *Chem. Eng. J.*, 2015, **267**, 132–141.

63 S. L. Shenoy, W. D. Bates, H. L. Frisch and G. E. Wnek, *Polymer*, 2005, **46**, 3372–3384.

64 C. Kriegel, A. Arrechi, K. Kit, D. J. McClements and J. Weiss, *Crit. Rev. Food Sci. Nutr.*, 2008, **48**, 775–797.

65 G. Doğan, F. Özyildiz, G. Basal and A. Uzel, *Int. Polym. Process.*, 2013, **28**, 143–150.

66 M. Pakravan, M. C. Heuzey and A. Ajji, *Polymer*, 2011, **52**, 4813–4824.

67 M. Z. Elsabee, H. F. Naguib and R. E. Morsi, *Mater. Sci. Eng., C*, 2012, **32**, 1711–1726.

68 P. Denis, M. Wrzecionek, A. Gadomska-Gajadhur and P. Sajkiewicz, *Polymers*, 2019, **11**, 2113.

69 D. Han and K. C. Cheung, *Polymers*, 2011, **3**, 1684–1733.

70 R. Rošic, J. Pelipenko, P. Kocbek, S. Baumgartner, M. Bešter-Rogač and J. Kristl, *Eur. Polym. J.*, 2012, **48**, 1374–1384.

71 X. Geng, O. H. Kwon and J. Jang, *Biomaterials*, 2005, **26**, 5427–5432.

72 N. Bhattarai, D. Edmondson, O. Veiseh, F. A. Matsen and M. Zhang, *Biomaterials*, 2005, **26**, 6176–6184.

73 M. T. M. Bizarria, M. A. D'Ávila and L. H. I. Mei, *Braz. J. Chem. Eng.*, 2014, **31**, 57–68.

74 S. Haider, Y. Al-Zeghayer, F. A. Ahmed Ali, A. Haider, A. Mahmood, W. A. Al-Masry, M. Imran and M. O. Aijaz, *J. Polym. Res.*, 2013, **20**, 105.

75 Y. P. Singh, S. Dasgupta, S. Nayar and R. Bhaskar, *J. Biomater. Sci., Polym. Ed.*, 2020, **31**, 781–803.

76 B. Kannan, H. Cha and I. C. Hosie, *Nano-Size Polym. Prep. Prop. Appl.*, 2016, 309–342.

77 G. Zhao, X. Zhang, T. J. Lu and F. Xu, *Adv. Funct. Mater.*, 2015, **25**, 5726–5738.

78 A. Barhoum, K. Pal, H. Rahier, H. Uludag, I. S. Kim and M. Bechelany, *Appl. Mater. Today*, 2019, **17**, 1–35.

79 Z. Zhang and X. J. Wang, *Quant. Biol.*, 2017, **5**, 136–142.

80 R. Rasouli, A. Barhoum, M. Bechelany and A. Dufresne, *Macromol. Biosci.*, 2019, **19**, 1800256.

81 A. Nayl, A. Abd-Elhamid, N. Awwad, M. Abdelgawad, J. Wu, X. Mo, S. Gomha, A. Aly and S. Brase, *Polymers*, 2022, **14**, 1508.

82 E. Ekrami, M. Khodabandeh Shahraky, M. Mahmoudifard, M. S. Mirtaleb and P. Shariati, *Int. J. Polym. Mater. Polym. Biomater.*, 2022, 1–15.

83 S. P. Miguel, D. R. Figueira, D. Simões, M. P. Ribeiro, P. Coutinho, P. Ferreira and I. J. Correia, *Colloids Surf., B*, 2018, **169**, 60–71.

84 M. Zahiri, M. Khanmohammadi, A. Goodarzi, S. Ababzadeh, M. Sagharjoghi Farahani, S. Mohandesnezhad, N. Bahrami, I. Nabipour and J. Ai, *Int. J. Biol. Macromol.*, 2020, **153**, 1241–1250.

85 J. B. Moreira, L. T. Lim, E. da, R. Zavareze, A. R. G. Dias, J. A. V. Costa and M. G. de Morais, *Food Hydrocolloids*, 2019, **93**, 131–136.

86 R. E. Ghitescu, A. M. Popa, A. Schipanski, C. Hirsch, G. Yazgan, V. I. Popa, R. M. Rossi, K. Maniura-Weber and G. Fortunato, *Eur. J. Pharm. Biopharm.*, 2018, **122**, 78–86.

87 P. Wang, Y. Li, C. Zhang, F. Feng and H. Zhang, *Food Chem.*, 2020, **308**, 125599.

88 B. S. Isik, F. Altay and E. Capanoglu, *Food Chem.*, 2018, **265**, 260–273.

89 B. Vafania, M. Fathi and S. Soleimanian-Zad, *Food Bioprod. Process.*, 2019, **116**, 240–248.

90 M. A. Dehcheshmeh and M. Fathi, *Int. J. Biol. Macromol.*, 2019, **122**, 272–279.

91 K. J. Figueroa-Lopez, J. L. Castro-Mayorga, M. M. Andrade-Mahecha, L. Cabedo and J. M. Lagaron, *Nanomaterials*, 2018, **8**, 199.

92 J. Pelipenko, P. Kocbek and J. Kristl, *Int. J. Pharm.*, 2015, **484**, 57–74.

93 M. Abrigo, S. L. McArthur and P. Kingshott, *Macromol. Biosci.*, 2014, **14**, 772–792.

94 A. Morie, T. Garg, A. K. Goyal and G. Rath, *Artif. Cells, Nanomed., Biotechnol.*, 2016, **44**, 135–143.

95 T. Subbiah, G. S. Bhat, R. W. Tock, S. Parameswaran and S. S. Ramkumar, *J. Appl. Polym. Sci.*, 2005, **96**, 557–569.

96 R. Langer, *Acc. Chem. Res.*, 2000, **33**, 94–101.

97 S. Frokjaer and D. E. Otzen, *Nat. Rev. Drug Discovery*, 2005, **4**, 298–306.

98 C. Shin, G. G. Chase and D. H. Reneker, *AIChE J.*, 2005, **51**, 3109–3113.

99 M. George and T. E. Abraham, *J. Controlled Release*, 2006, **114**, 1–14.

100 Z. Wang, C. Zhao and Z. Pan, *J. Colloid Interface Sci.*, 2015, **441**, 121–129.

101 K. M. Yun, C. J. Hogan, Y. Matsubayashi, M. Kawabe, F. Iskandar and K. Okuyama, *Chem. Eng. Sci.*, 2007, **62**, 4751–4759.

102 J. Širc, R. Hobzová, N. Kostina, M. Munzarová, M. Juklíčková, M. Lhotka, Š. Kubinová, A. Zajícová and J. Michálek, *J. Nanomater.*, 2012, **2012**, 1–14.

103 E. Biazar, D. Zaeifi, S. H. Keshel, S. Ojani, A. Hajiaghaee, R. Safarpour, M. Sheikholeslami, B. Heidari and S. Sadeghpour, *J. Paramed. Sci.*, 2015, **6**, 46–51.

104 S. Deepthi, J. Venkatesan, S. K. Kim, J. D. Bumgardner and R. Jayakumar, *Int. J. Biol. Macromol.*, 2016, **93**, 1338–1353.

105 E. J. Chong, T. T. Phan, I. J. Lim, Y. Z. Zhang, B. H. Bay, S. Ramakrishna and C. T. Lim, *Acta Biomater.*, 2007, **3**, 321–330.

106 A. E. Donius, M. A. Kiechel, C. L. Schauer and U. G. K. Wegst, *J. R. Soc., Interface*, 2013, **10**, 20120946.

107 Z. Li, W. Hu, Y. Zhao, L. Ren and X. Yuan, *Colloids Surf., B*, 2018, **169**, 151–159.

108 W. A. Sarhan and H. M. E. Azzazy, *Carbohydr. Polym.*, 2015, **122**, 135–143.

109 M. Kumorek, I. M. Minisy, T. Krunclová, M. Voršiláková, K. Venclíková, E. M. Chánová, O. Janoušková and D. Kubies, *Mater. Sci. Eng., C*, 2020, **109**, 110493.

110 J. Huang, Y. Cheng, Y. Wu, X. Shi, Y. Du and H. Deng, *Int. J. Biol. Macromol.*, 2019, **139**, 191–198.

111 X. Feng, X. Hou, C. Cui, S. Sun, S. Sadik, S. Wu and F. Zhou, *Eng. Regen.*, 2021, **2**, 57–62.

112 M. A. Kiechel and C. L. Schauer, *Carbohydr. Polym.*, 2013, **95**, 123–133.

113 L. Wang, H. Lv, L. Liu, Q. Zhang, P. Nakielski, Y. Si, J. Cao, X. Li, F. Pierini, J. Yu and B. Ding, *J. Colloid Interface Sci.*, 2020, **565**, 416–425.

114 C. Wu, H. Su, A. Karydis, K. M. Anderson, N. Ghadri, S. Tang, Y. Wang and J. D. Bumgardner, *Biomed. Mater.*, 2017, **13**, 015004.

115 R. Jayakumar, N. Nwe, S. Tokura and H. Tamura, *Int. J. Biol. Macromol.*, 2007, **40**, 175–181.

116 I. Aranaz, A. R. Alcántara, M. C. Civera, C. Arias, B. Elorza, A. H. Caballero and N. Acosta, *Polymers*, 2021, **13**, 3256.

117 N. Islam, I. Dmour and M. O. Taha, *Heliyon*, 2019, **5**, e01684.

118 J. A. Jennings, *Chitosan Based Biomater.*, 2017, **1**, 159–182.

119 T. Kean and M. Thanou, *Adv. Drug Delivery Rev.*, 2010, **62**, 3–11.

120 S. K. Kim and N. Rajapakse, *Carbohydr. Polym.*, 2005, **62**, 357–368.

121 I. Y. Kim, S. J. Seo, H. S. Moon, M. K. Yoo, I. Y. Park, B. C. Kim and C. S. Cho, *Biotechnol. Adv.*, 2008, **26**, 1–21.

122 Y. Tang, X. Lan, C. Liang, Z. Zhong, R. Xie, Y. Zhou, X. Miao, H. Wang and W. Wang, *Carbohydr. Polym.*, 2019, **219**, 113–120.

123 J. Becerra, M. Rodriguez, D. Leal, K. Noris-Suarez and G. Gonzalez, *J. Mater. Sci.: Mater. Med.*, 2022, **33**, 1–16.

124 I. Kohsari, Z. Shariatinia and S. M. Pourmortazavi, *Carbohydr. Polym.*, 2016, **140**, 287–298.

125 Y. Zhong, B. A. Bauer and S. Patel, *J. Comput. Chem.*, 2011, **32**, 3339–3353.

126 R. G. Boot, E. F. C. Blommaart, E. Swart, K. Ghauharali-van der Vlugt, N. Bijl, C. Moe, A. Place and J. M. F. G. Aerts, *J. Biol. Chem.*, 2001, **276**, 6770–6778.

127 H. Zhang and S. H. Neau, *Biomaterials*, 2001, **22**, 1653–1658.

128 L. Xia, S. Wang, Z. Jiang, J. Chi, S. Yu, H. Li, Y. Zhang, L. Li, C. Zhou, W. Liu and B. Han, *Carbohydr. Polym.*, 2021, **264**, 117965.

129 S. Ma, A. Adayi, Z. Liu, M. Li, M. Wu, L. Xiao, Y. Sun, Q. Cai, X. Yang, X. Zhang and P. Gao, *Sci. Rep.*, 2016, **6**, 1–10.

130 S. Torkaman, H. Rahmani, A. Ashori and S. H. M. Najafi, *Carbohydr. Polym.*, 2021, **258**, 117675.

131 L. Casettari, D. Vllasaliu, J. K. W. Lam, M. Soliman and L. Illum, *Biomaterials*, 2012, **33**, 7565–7583.

132 B. P. Antunes, A. F. Moreira, V. M. Gaspar and I. J. Correia, *Carbohydr. Polym.*, 2015, **130**, 104–112.

133 G. Sabarees, V. Velmurugan, G. P. Tamilarasi, V. Alagarsamy and V. Raja Solomon, *Polymers*, 2022, **14**, 3994.

134 M. Ignatova, N. Manolova and I. Rashkov, *Macromol. Biosci.*, 2013, **13**, 860–872.

135 S. Alven, B. Buyana, Z. Feketshane and B. A. Aderibigbe, *Pharmaceutics*, 2021, **13**, 964.

136 H. Penchev, D. Paneva, N. Manolova and I. Rashkov, *Macromol. Biosci.*, 2009, **9**, 884–894.

137 C. Tan, J. Wang and B. Sun, *Biotechnol. Adv.*, 2021, **48**, 107727.

138 N. Monteiro, M. Martins, A. Martins, N. A. Fonseca, J. N. Moreira, R. L. Reis and N. M. Neves, *Acta Biomater.*, 2015, **18**, 196–205.

139 A. Neamnark, R. Rujiravanit and P. Supaphol, *Carbohydr. Polym.*, 2006, **66**, 298–305.

140 A. Vijayan, A. Sabareeswaran and G. S. V. Kumar, *Sci. Rep.*, 2019, **9**, 19165.

141 S. M. Alipour, M. Nouri, J. Mokhtari and S. H. Bahrami, *Carbohydr. Res.*, 2009, **344**, 2496–2501.

142 M. Ignatova, N. Manolova and I. Rashkov, *Eur. Polym. J.*, 2007, **43**, 1112–1122.

143 M. E. Abd El-Hack, M. T. El-Saadony, M. E. Shafi, N. M. Zabermawi, M. Arif, G. E. Batiha, A. F. Khafaga, Y. M. Abd El-Hakim and A. A. Al-Sagheer, *Int. J. Biol. Macromol.*, 2020, **164**, 2726–2744.

144 Z. Shariatinia, *Int. J. Biol. Macromol.*, 2018, **120**, 1406–1419.

145 Z. G. Chen, P. W. Wang, B. Wei, X. M. Mo and F. Z. Cui, *Acta Biomater.*, 2010, **6**, 372–382.

146 N. Cai, C. Li, C. Han, X. Luo, L. Shen, Y. Xue and F. Yu, *Appl. Surf. Sci.*, 2016, **369**, 492–500.

147 D. N. Phan, H. Lee, B. Huang, Y. Mukai and I. S. Kim, *Cellulose*, 2019, **26**, 1781–1793.

148 P. Bösiger, I. M. T. Richard, L. Le Gat, B. Michen, M. Schubert, R. M. Rossi and G. Fortunato, *Carbohydr. Polym.*, 2018, **186**, 122–131.

149 Y. T. Jia, J. Gong, X. H. Gu, H. Y. Kim, J. Dong and X. Y. Shen, *Carbohydr. Polym.*, 2007, **67**, 403–409.

150 P. Zou, W. H. Lee, Z. Gao, D. Qin, Y. Wang, J. Liu, T. Sun and Y. Gao, *Carbohydr. Polym.*, 2020, **232**, 115786.

151 L. Van Der Schueren, I. Steyaert, B. De Schoenmaker and K. De Clerck, *Carbohydr. Polym.*, 2012, **88**, 1221–1226.

152 D. Semnani, E. Naghashzargar, M. Hadjianfar, F. Dehghan Manshadi, S. Mohammadi, S. Karbasi and F. Effaty, *Int. J. Polym. Mater. Polym. Biomater.*, 2017, **66**, 149–157.

153 J. E. Ko, Y. G. Ko, W. Il Kim, O. K. Kwon and O. H. Kwon, *J. Biomed. Mater. Res., Part B*, 2017, **105**, 1906–1915.

154 D. R. Bienek, K. M. Hoffman and W. Tutak, *J. Mater. Sci.: Mater. Med.*, 2016, **27**, 146.

155 S. L. Levengood, A. E. Erickson, F. Chien Chang and M. Zhang, *J. Mater. Chem. B*, 2017, **5**, 1822–1833.

156 S. Gomes, G. Rodrigues, G. Martins, C. Henriques and J. C. Silva, *Int. J. Biol. Macromol.*, 2017, **102**, 1174–1185.

157 A. Madni, R. Khan, M. Ikram, S. S. Naz, T. Khan and F. Wahid, *Int. J. Polym. Sci.*, 2019, **2019**, 1–8.

158 T. Prasad, E. A. Shabeena, D. Vinod, T. V. Kumary and P. R. Anil Kumar, *J. Mater. Sci.: Mater. Med.*, 2015, **26**, 1–13.

159 C. Tangsadthakun, S. Kanokpanont, N. Sanchavanakit, T. Banaprasert and S. Damrongsakkul, *J. Met., Mater. Miner.*, 2017, **16**, 37–44.

160 M. Pezeshki-Modaress, M. Zandi and S. Rajabi, *Prog. Biomater.*, 2018, **7**, 207–218.

161 X. Jing, H. Y. Mi, X. C. Wang, X. F. Peng and L. S. Turng, *ACS Appl. Mater. Interfaces*, 2015, **7**, 6955–6965.

162 S. Kar, T. Kaur and A. Thirugnanam, *Int. J. Biol. Macromol.*, 2016, **82**, 628–636.

163 Y. Lei, Z. Xu, Q. Ke, W. Yin, Y. Chen, C. Zhang and Y. Guo, *Mater. Sci. Eng., C*, 2017, **72**, 134–142.

164 X. Li, H. M. Yin, K. Su, G. Sen Zheng, C. Y. Mao, W. Liu, P. Wang, Z. Zhang, J. Z. Xu, Z. M. Li and G. Q. Liao, *ACS Biomater. Sci. Eng.*, 2019, **5**, 2998–3006.

165 S. P. Mallick, K. Pal, A. Rastogi and P. Srivastava, *Des. Monomers Polym.*, 2016, **19**, 271–282.

166 D. Sadeghi, S. Karbasi, S. Razavi, S. Mohammadi, M. A. Shokrgozar and S. Bonakdar, *J. Appl. Polym. Sci.*, 2016, **133**, 44171.

167 V. Vishwanath, K. Pramanik and A. Biswas, *J. Biomater. Sci., Polym. Ed.*, 2016, **27**, 657–674.

168 S. P. Mallick, B. N. Singh, A. Rastogi and P. Srivastava, *Int. J. Biol. Macromol.*, 2018, **112**, 909–920.

169 A. Kaviani, S. M. Zebarjad, S. Javadpour, M. Ayatollahi and R. Bazargan-Lari, *Int. J. Polym. Anal. Charact.*, 2019, **24**, 191–203.

170 J. M. Chupa, A. M. Foster, S. R. Sumner, S. V. Madihally and H. W. T. Matthew, *Biomaterials*, 2000, **21**, 2315–2322.

171 L. Zhang, Q. Ao, A. Wang, G. Lu, L. Kong, Y. Gong, N. Zhao and X. Zhang, *J. Biomed. Mater. Res., Part A*, 2006, **77**, 277–284.

172 C. Huang, R. Chen, Q. Ke, Y. Morsi, K. Zhang and X. Mo, *Colloids Surf., B*, 2011, **82**, 307–315.

173 F. Du, H. Wang, W. Zhao, D. Li, D. Kong, J. Yang and Y. Zhang, *Biomaterials*, 2012, **33**, 762–770.

174 R. V. Badhe, D. Bijukumar, D. R. Chejara, M. Mabrouk, Y. E. Choonara, P. Kumar, L. C. du Toit, P. P. D. Kondiah and V. Pillay, *Carbohydr. Polym.*, 2017, **157**, 1215–1225.

175 A. C. Akman, R. S. Tiğli, M. Gumusderelioglu and R. M. Nohutcu, *J. Biomed. Mater. Res., Part A*, 2010, **92**, 953–962.

176 R. Shen, W. Xu, Y. Xue, L. Chen, H. Ye, E. Zhong, Z. Ye, J. Gao and Y. Yan, *Artif. Cells, Nanomed., Biotechnol.*, 2018, **46**, 419–430.

177 S. Wang, W. Liu, B. Han and L. Yang, *Appl. Surf. Sci.*, 2009, **255**, 8701–8705.

178 Y. Liang, W. Liu, B. Han, C. Yang, Q. Ma, W. Zhao, M. Rong and H. Li, *J. Mater. Sci.: Mater. Med.*, 2011, **22**, 175–183.

179 L. Guan, L. Ge, X. Tang, S. Su, P. Tian, N. Xiao, H. Zhang, L. Zhang and P. Liu, *Cells Tissues Organs*, 2013, **198**, 190–197.

180 Y. H. Wang, T. H. Young and T. J. Wang, *Exp. Eye Res.*, 2019, **185**, 107679.

181 I. Doench, M. E. W. Torres-Ramos, A. Montembault, P. N. de Oliveira, C. Halimi, E. Viguier, L. Heux, R. Siadous, R. M. S. M. Thiré and A. Osorio-Madrazo, *Polymers*, 2018, **10**, 1202.

182 I. Doench, T. A. Tran, L. David, A. Montembault, E. Viguier, C. Gorzelanny, G. Sudre, T. Cachon, M. Louback-Mohamed, N. Horbelt, C. Peniche-Covas and A. Osorio-Madrazo, *Biomimetics*, 2019, **4**, 19.

183 D. Yuan, Z. Chen, X. Xiang, S. Deng, K. Liu, D. Xiao, L. Deng and G. Feng, *J. Biomed. Mater. Res., Part B*, 2019, **107**, 2305–2316.

184 Z. Wang, Q. Hu and L. Cai, *Int. J. Polym. Sci.*, 2010, **2010**, 1–7.

185 X. M. Pu, Z. Z. Sun, Z. Q. Hou, Y. Yang, Q. Q. Yao and Q. Q. Zhang, *J. Biomed. Mater. Res., Part B*, 2012, 1179–1189.

186 B. Balakrishnan, D. Soman, U. Payanam, A. Laurent, D. Labarre and A. Jayakrishnan, *Acta Biomater.*, 2017, **53**, 343–354.

187 C. P. Jiménez-Gómez, J. A. Cecilia, M. Guidotti and R. Soengas, *Molecules*, 2020, **25**, 3981.

188 F. Ding, H. Deng, Y. Du, X. Shi and Q. Wang, *Nanoscale*, 2014, **6**, 9477–9493.

189 W. A. Sarhan, H. M. E. Azzazy and I. M. El-Sherbiny, *ACS Appl. Mater. Interfaces*, 2016, **8**, 6379–6390.

190 R. Jayakumar, M. Prabaharan, P. T. Sudheesh Kumar, S. V. Nair and H. Tamura, *Biotechnol. Adv.*, 2011, **29**, 322–337.

191 N. Ardila, N. Medina, M. Arkoun, M. C. Heuzey, A. Ajji and C. J. Panchal, *Cellulose*, 2016, **23**, 3089–3104.

192 Y. Zhou, Q. Dong, H. Yang, X. Liu, X. Yin, Y. Tao, Z. Bai and W. Xu, *Carbohydr. Polym.*, 2017, **168**, 220–226.

193 A. C. Alavarse, F. W. de Oliveira Silva, J. T. Colque, V. M. da Silva, T. Prieto, E. C. Venancio and J. J. Bonvent, *Mater. Sci. Eng., C*, 2017, **77**, 271–281.

194 A. Ehterami, M. Salehi, S. Farzamfar, A. Vaez, H. Samadian, H. Sahrapeyma, M. Mirzaii, S. Ghorbani and A. Goodarzi, *Int. J. Biol. Macromol.*, 2018, **117**, 601–609.

195 S. Fahimirad, H. Abtahi, P. Satei, E. Ghaznavi-Rad, M. Moslehi and A. Ganji, *Carbohydr. Polym.*, 2021, **259**, 117640.

196 L. Zhou, L. Cai, H. Ruan, L. Zhang, J. Wang, H. Jiang, Y. Wu, S. Feng and J. Chen, *Int. J. Biol. Macromol.*, 2021, **183**, 1145–1154.

197 X. Li, C. Wang, S. Yang, P. Liu and B. Zhang, *Int. J. Nanomed.*, 2018, **13**, 5287–5299.

198 N. Charernsriwilaiwat, T. Rojanarata, T. Ngawhirunpat, M. Sukma and P. Opanasopit, *Int. J. Pharm.*, 2013, **452**, 333–343.

199 C. Mouro, M. Simões, I. C. Gouveia and B. Xu, *Adv. Polym. Technol.*, 2019, **2019**, 1–11.

200 I. Yousefi, M. Pakravan, H. Rahimi, A. Bahador, Z. Farshadzadeh and I. Haririan, *Mater. Sci. Eng., C*, 2017, **75**, 433–444.

201 N. T. Ardekani, M. Khorram, K. Zomorodian, S. Yazdanpanah, H. Veisi and H. Veisi, *Int. J. Biol. Macromol.*, 2019, **125**, 743–750.

202 K. Kataria, A. Gupta, G. Rath, R. B. Mathur and S. R. Dhakate, *Int. J. Pharm.*, 2014, **469**, 102–110.

203 H. R. Bakhsheshi-Rad, A. F. Ismail, M. Aziz, M. Akbari, Z. Hadisi, M. Omidi and X. Chen, *Int. J. Biol. Macromol.*, 2020, **149**, 513–521.

204 H. Iqbal, B. A. Khan, Z. U. Khan, A. Razzaq, N. U. Khan, B. Menaa and F. Menaa, *Int. J. Biol. Macromol.*, 2020, **144**, 921–931.

205 R. Ahmed, M. Tariq, I. Ali, R. Asghar, P. Noorunnisa Khanam, R. Augustine and A. Hasan, *Int. J. Biol. Macromol.*, 2018, **120**, 385–393.

206 L. Sun, J. Han, Z. Liu, S. Wei, X. Su and G. Zhang, *J. Photochem. Photobiol., B*, 2019, **197**, 111539.

207 B. P. Antunes, A. F. Moreira, V. M. Gaspar and I. J. Correia, *Carbohydr. Polym.*, 2015, **130**, 104–112.

208 Z. X. Cai, X. M. Mo, K. H. Zhang, L. P. Fan, A. L. Yin, C. L. He and H. S. Wang, *Int. J. Mol. Sci.*, 2010, **11**, 3529–3539.

209 R. Zhao, X. Li, B. Sun, Y. Zhang, D. Zhang, Z. Tang, X. Chen and C. Wang, *Int. J. Biol. Macromol.*, 2014, **68**, 92–97.

210 B. Poornima and P. S. Korrapati, *Carbohydr. Polym.*, 2017, **157**, 1741–1749.

211 N. Mahmoudi and A. Simchi, *Mater. Sci. Eng., C*, 2017, **70**, 121–131.

212 T. T. Yuan, A. M. DiGeorge Foushee, M. C. Johnson, A. R. Jockheck-Clark and J. M. Stahl, *Nanoscale Res. Lett.*, 2018, **13**, 88.

213 S. Datta, A. P. Rameshbabu, K. Bankoti, P. P. Maity, D. Das, S. Pal, S. Roy, R. Sen and S. Dhara, *ACS Biomater. Sci. Eng.*, 2017, **3**, 1738–1749.

214 S. Yang, X. Han, Y. Jia, H. Zhang and T. Tang, *Polymers*, 2017, **9**, 697.

215 A. Chanda, J. Adhikari, A. Ghosh, S. R. Chowdhury, S. Thomas, P. Datta and P. Saha, *Int. J. Biol. Macromol.*, 2018, **116**, 774–785.

216 P. Nakielski and F. Pierini, *Acta Biomater.*, 2019, **84**, 63–76.

217 J. Huang, Y. Cheng, Y. Wu, X. Shi, Y. Du and H. Deng, *Int. J. Biol. Macromol.*, 2019, **139**, 191–198.

218 L. Wang, H. Lv, L. Liu, Q. Zhang, P. Nakielski, Y. Si, J. Cao, X. Li, F. Pierini, J. Yu and B. Ding, *J. Colloid Interface Sci.*, 2020, **565**, 416–425.

219 P. Sasmal and P. Datta, *J. Drug Delivery Sci. Technol.*, 2019, **52**, 559–567.

220 H. Thomas, J. Diamond, A. Vieco, S. Chaudhuri, E. Shinnar, S. Cromer, P. Perel, G. A. Mensah, J. Narula, C. O. Johnson, G. A. Roth and A. E. Moran, *Glob. Heart*, 2018, **13**, 143–163.

221 J. Zhang, W. Xia, P. Liu, Q. Cheng, T. Tahirou, W. Gu and B. Li, *Mar. Drugs*, 2010, **8**, 1962–1987.

222 H. J. Jin, H. Zhang, M. L. Sun, B. G. Zhang and J. W. Zhang, *J. Thromb. Thrombolysis*, 2013, **36**, 458–468.

223 J. Liao, X. Ren, B. Yang, H. Li, Y. Zhang and Z. Yin, *Drug Dev. Ind. Pharm.*, 2019, **45**, 88–95.

224 F. Du, H. Wang, W. Zhao, D. Li, D. Kong, J. Yang and Y. Zhang, *Biomaterials*, 2012, **33**, 762–770.

225 S. Hirano and Y. Noishiki, *J. Biomed. Mater. Res.*, 1985, **19**, 413–417.

226 S. Preethi Soundarya, A. Haritha Menon, S. Viji Chandran and N. Selvamurugan, *Int. J. Biol. Macromol.*, 2018, **119**, 1228–1239.

227 J. Nourmohammadi, A. Ghaee and S. H. Liavali, *Carbohydr. Polym.*, 2016, **138**, 172–179.

228 Y. Zhang, J. R. Venugopal, A. El-Turki, S. Ramakrishna, B. Su and C. T. Lim, *Biomaterials*, 2008, **29**, 4314–4322.

229 K. A. Chan, S. E. Andrade, M. Boles, D. S. M. Buist, G. A. Chase, J. G. Donahue, M. J. Goodman, J. H. Gurwitz, A. Z. Lacroix and R. Platt, *Lancet*, 2000, **355**, 2185–2188.

230 N. Ghadri, K. M. Anderson, P. Adatrow, S. H. Stein, H. Su, F. Garcia-Godoy, A. Karydis and J. D. Bumgardner, *J. Biomater. Nanobiotechnol.*, 2018, **09**, 210–231.

231 C. Wu, H. Su, A. Karydis, K. M. Anderson, N. Ghadri, S. Tang, Y. Wang and J. D. Bumgardner, *Biomed. Mater.*, 2017, **13**, 015004.

232 S. Jin, J. Li, J. Wang, J. Jiang, Y. Zuo, Y. Li and F. Yang, *Int. J. Nanomed.*, 2018, **13**, 4591–4605.

233 M. Masoudi Rad, S. Nouri Khorasani, L. Ghasemi-Mobarakeh, M. P. Prabhakaran, M. R. Foroughi, M. Kharaziha, N. Saadatkish and S. Ramakrishna, *Mater. Sci. Eng., C*, 2017, **80**, 75–87.

234 F. Sharifi, S. M. Atyabi, D. Norouzian, M. Zandi, S. Irani and H. Bakhshi, *Int. J. Biol. Macromol.*, 2018, **115**, 243–248.

235 A. Pangon, S. Saesoo, N. Saengkrit, U. Ruktanonchai and V. Intasanta, *Carbohydr. Polym.*, 2016, **144**, 419–427.

236 T. A. Gaziano, *Circulation*, 2005, **112**, 3547–3553.

237 T. A. Gaziano, *Health Aff.*, 2007, **26**, 13–24.

238 Y. Naito, T. Shinoka, D. Duncan, N. Hibino, D. Solomon, M. Cleary, A. Rathore, C. Fein, S. Church and C. Breuer, *Adv. Drug Delivery Rev.*, 2011, **63**, 312–323.

239 M. A. Cleary, E. Geiger, C. Grady, C. Best, Y. Naito and C. Breuer, *Trends Mol. Med.*, 2012, **18**, 394–404.

240 V. Catto, S. Farè, G. Freddi and M. C. Tanzi, *ISRN Vasc. Med.*, 2014, 1–27.

241 S. Li, D. Sengupta and S. Chien, *Wiley Interdiscip. Rev.: Syst. Biol. Med.*, 2014, **6**, 61–76.

242 D. G. Seifu, A. Purnama, K. Mequanint and D. Mantovani, *Nat. Rev. Cardiol.*, 2013, **10**, 410–421.

243 S. L. Mitchell and L. E. Niklason, *Cardiovasc. Pathol.*, 2003, **12**, 59–64.

244 C. P. Barnes, S. A. Sell, E. D. Boland, D. G. Simpson and G. L. Bowlin, *Adv. Drug Delivery Rev.*, 2007, **59**, 1413–1433.

245 A. Nieponice, L. Soletti, J. Guan, B. M. Deasy, J. Huard, W. R. Wagner and D. A. Vorp, *Biomaterials*, 2008, **29**, 825–833.

246 H. Kurobe, M. W. Maxfield, C. K. Breuer and T. Shinoka, *Stem Cells Transl. Med.*, 2012, **1**, 566–571.

247 D. R. Duncan and C. K. Breuer, *Vasc. Cell*, 2011, **3**, 23.

248 J. Venugopal, Y. Z. Zhang and S. Ramakrishna, *Nanotechnology*, 2005, **16**, 2138–2142.

249 S. J. Lee, J. J. Yoo, G. J. Lim, A. Atala and J. Stitzel, *J. Biomed. Mater. Res., Part A*, 2007, **83**, 999–1008.

250 H. Liu, X. Li, G. Zhou, H. Fan and Y. Fan, *Biomaterials*, 2011, **32**, 3784–3793.

251 M. Li, M. J. Mondrinos, M. R. Gandhi, F. K. Ko, A. S. Weiss and P. I. Lelkes, *Biomaterials*, 2005, **26**, 5999–6008.

252 C. Xu, R. Inai, M. Kotaki and S. Ramakrishna, *Tissue Eng.*, 2004, **10**, 1160–1168.

253 F. Yang, R. Murugan, S. Wang and S. Ramakrishna, *Biomaterials*, 2005, **26**, 2603–2610.

254 T. Wang, X. Ji, L. Jin, Z. Feng, J. Wu, J. Zheng, H. Wang, Z. W. Xu, L. Guo and N. He, *ACS Appl. Mater. Interfaces*, 2013, **5**, 3757–3763.

255 C. E. Schmidt and J. B. Leach, *Annu. Rev. Biomed. Eng.*, 2003, **5**, 293–347.

256 G. A. A. Saracino, D. Cigognini, D. Silva, A. Caprini and F. Gelain, *Chem. Soc. Rev.*, 2013, **42**, 225–262.

257 A. Subramanian, U. M. Krishnan and S. Sethuraman, *J. Biomed. Sci.*, 2009, **16**, 108.

258 H. Cao, T. Liu and S. Y. Chew, *Adv. Drug Delivery Rev.*, 2009, **61**, 1055–1064.

259 S. M. Willerth and S. E. Sakiyama-Elbert, *Adv. Drug Delivery Rev.*, 2007, **59**, 325–338.

260 J. Y. Lee, C. A. Bashur, A. S. Goldstein and C. E. Schmidt, *Biomaterials*, 2009, **30**, 4325–4335.

261 L. Ghasemi-Mobarakeh, M. P. Prabhakaran, M. Morshed, M. H. Nasr-Esfahani and S. Ramakrishna, *Biomaterials*, 2008, **29**, 4532–4539.

262 M. P. Prabhakaran, J. R. Venugopal, T. Ter Chyan, L. B. Hai, C. K. Chan, A. Y. Lim and S. Ramakrishna, *Tissue Eng., Part A*, 2008, **14**, 1787–1797.

263 F. M. Kievit, A. Cooper, S. Jana, M. C. Leung, K. Wang, D. Edmondson, D. Wood, J. S. H. Lee, R. G. Ellenbogen and M. Zhang, *Adv. Healthcare Mater.*, 2013, **2**, 1651–1659.

264 J. Xie, X. Li, J. Lipner, C. N. Manning, A. G. Schwartz, S. Thomopoulos and Y. Xia, *Nanoscale*, 2010, **2**, 923–926.

265 A. Cooper, N. Bhattarai and M. Zhang, *Carbohydr. Polym.*, 2011, **85**, 149–156.

266 A. Cooper, C. Zhong, Y. Kinoshita, R. S. Morrison, M. Rolandi and M. Zhang, *J. Mater. Chem.*, 2012, **22**, 3105–3109.

267 M. Wieckiewicz, K. Boening, N. Grychowska and A. Paradowska-Stolarz, *Mini-Rev. Med. Chem.*, 2016, **17**, 401–409.

268 I. Aranaz, N. Acosta, C. Civera, B. Elorza, J. Mingo, C. Castro, M. de Los, L. Gandía and A. H. Caballero, *Polymers*, 2018, **10**, 213.

269 C. R. Afonso, R. S. Hirano, A. L. Gaspar, E. G. L. Chagas, R. A. Carvalho, F. V. Silva, G. R. Leonardi, P. S. Lopes, C. F. Silva and C. M. P. Yoshida, *Int. J. Biol. Macromol.*, 2019, **132**, 1262–1273.

270 C. S. Kong, J. A. Kim, B. Ahn, H. G. Byun and S. K. Kim, *Process Biochem.*, 2010, **45**, 179–186.

271 E. M. Costa, S. Silva, A. R. Madureira, A. Cardelle-Cobas, F. K. Tavaria and M. M. Pintado, *Carbohydr. Polym.*, 2014, **101**, 1081–1086.

272 A. H. M. Resende, J. M. Farias, D. D. B. Silva, R. D. Rufino, J. M. Luna, T. C. M. Stamford and L. A. Sarubbo, *Colloids Surf., B*, 2019, **181**, 77–84.

273 A. Sionkowska, M. Michalska-Sionkowska and M. Walczak, *Int. J. Biol. Macromol.*, 2020, **149**, 290–295.

274 P. Morganti, P. Del Ciotto, F. Carezzi, M. L. Nunziata and G. Morganti, *Nanomater. Regen. Med.*, 2016, 123–142.

275 X. J. Huang, D. Ge and Z. K. Xu, *Eur. Polym. J.*, 2007, **43**, 3710–3718.

276 K. Desai, K. Kit, J. Li, P. Michael Davidson, S. Zivanovic and H. Meyer, *Polymer*, 2009, **50**, 3661–3669.

277 S. Haider and S. Y. Park, *J. Membr. Sci.*, 2009, **328**, 90–96.

278 W. S. Wan Ngah, C. S. Endud and R. Mayanar, *React. Funct. Polym.*, 2002, **50**, 181–190.

279 B. Kannan, H. Cha and I. C. Hosie, *Nano-Size Polym. Prep. Prop. Appl.*, 2016, 309–342.